Application of Improved Honey Badger Algorithm in Multi-objective Reactive Power Optimization

Hongyu Long, Yuqiang He, Yongsheng He*, Chunyan Song, Qian Gao and Hao Tan

Abstract—**Multi-objective reactive power optimization (MORPO) is a high-dimensional, nonlinear, multi-constraint problem. To solve this problem, an improved multi-objective honey badger algorithm (MOIHBA) is proposed. To address the shortcomings of the original algorithm, such as easy falling into local optimum and insufficient population diversity, the improved algorithm introduces a sine chaotic mapping strategy to expand the population diversity, a backward learning mechanism to narrow the range of high-quality solution sets, and a cross-learning mechanism to improve the precision of the algorithm optimization process. In addition, in order to obtain the pareto optimal set (POS), a method based on calculating individual rank and crowding distance is proposed to sort the non-inferior solution, and the best compromise solution (BCS) is obtained by using a fuzzy theory strategy. By introducing three objective functions of active power loss, voltage stability index, and voltage deviation, the multi-objective reactive power optimization is established. To investigate the robustness of the introduced improved algorithm and its ability to solve the MORPO problem, this paper uses IEEE30, IEEE57, and IEEE118 as test systems that optimize the dual objective and triple objective simultaneously. In order to study the comprehensive performance of the improved algorithm, the algorithm time complexity, GD index, and HV index are adopted for evaluation. The simulation results and performance index results show that compared with other algorithms, MOIHBA has better BCS and pareto fronts (PFs) with the best uniformity and convergence. Therefore, the MOIHBA algorithm has a greater competitive advantage in solving the MORPO problem.**

Index Terms—**Honey badger algorithm, multi-objective, reactive power optimization, sine chaotic mapping strategy, cross-learning mechanism**

Hongyu Long is a professor level senior engineer at Chongqing Key Laboratory of Complex Systems and Bionic Control, Chongqing University of Posts and Telecommunications, Chongqing 400065, China (e-mail: longhongyu20@163.com).

Yuqiang He is a postgraduate student at Chongqing Key Laboratory of Complex Systems and Bionic Control, Chongqing University of Posts and Telecommunications, Chongqing 400065, China (e-mail: heyuqiang_cq@163.com).

Yongsheng He is a professor level senior engineer of State Grid Chongqing Electric Power Company, Chongqing 400015, China (corresponding author to provide phone: +8615922730078; e-mail: heyongsheng_bj@163.com).

Chunyan Song is a senior engineer of State Grid Zhejiang Electric Power Company, Zhejiang 310007, China (e-mail: songchunyan_zj@163.com).

Qian Gao is a senior engineer of State Grid Jiangsu Electric Power Company, Jiangsu 210000, China (e-mail: gaoqian_js@163.com).

Hao Tan is a senior engineer at the Economic and Technology Research Institute of State Grid Chongqing Electric Power Company, Chongqing 401120, China (e-mail: tanhao_cq@163.com).

I. INTRODUCTION

OVER the decades, with climate change and the development of power generation technology, the economy and security of the grid have encountered many challenges, including the grid's reactive power optimization (RPO) [1]. Reactive power optimization in the power system is a sub-problem of the optimal power flow (OPF) problem. From the perspective of voltage quality, the rational regulation of reactive power resources plays a great role in the power system's safety, economy, and stable operation. Therefore, it has received increasing attention from scholars. The main purpose of reactive power optimization is to achieve the goal of reducing active power losses, reducing voltage deviations, and enhancing voltage stability by coordinating and optimizing control variables, such as the voltage value of generators, the setting of transformer tap ratios, and the switching of reactive power compensation devices while satisfying equation constraints and inequality constraints [2]. Among them, the equivalence constraint refers to the power flow equation and the inequivalence constraint refers to the limits of operation and control parameters in the power system [3].

With the increase in the operational requirements of power systems and the increased objectives considered by decision-makers over recent years, the optimization problem has gradually evolved from a single-objective optimization problem to a multi-objective optimization problem in the field of reactive power optimization, which is of great significance for solving practical power system problems. The multi-objective reactive optimization problem includes continuous and discrete control variables, so it is again a multi-constrained, multi-variable, multi-objective mixed-integer nonlinear optimization problem [4,5]. To solve this problem, many scholars have proposed different solutions, which are mainly divided into two categories, one is a classic optimization technique and the other is an artificial intelligence technique. Traditional optimization methods include gradient method [6], interior point method [7], linear programming method and nonlinear programming method [8]. In solving multi-objective problems, traditional methods are used to convert multi-objective optimization problems into single-objective optimization problems by using weighting method [9], ε-constraint method, and fuzzy decision method [10]. On the one hand, these traditional methods can only be optimized for some specific goal functions and they have limitations in solving functions that are non-linear, non-convex, and discontinuous with constraints [11]. And on the other hand, the traditional

methods use a single-path optimization model, when the algorithm searches for the optimal value, it tends to converge to the local optimum rather than the global optimum [12]. On this basis, artificial intelligence algorithms have gradually emerged, and numerous scholars have attempted to solve the MORPO problem using such new intelligence algorithms. The representative algorithms are particle swarm algorithm (PSO) [13], sine cosine algorithm (SCA) [14], gravitational search algorithm (GSA) [15], imperialist competition algorithm (ICA) [16], differential evolution algorithm (DE) [17,18], cuckoo search algorithm (CS) [19-21], genetic algorithm (GA) [22], beetle antennae search algorithm (BAS) [23], NSGA-II algorithm [24], gray wolf optimization algorithm (GWO) [25,26] and bacterial foraging optimization algorithm (BFO) [27]. The results of this related literature show that the meta-heuristic algorithm is superior and more reliable than traditional methods in solving MORPO problems.

The honey badger algorithm (HBA) is a new intelligent algorithm proposed by Fatma A. Hashim in 2021 [28]. The HBA is characterized by fewer parameters, strong optimality finding ability and fast convergence. However, there are still some shortcomings in this algorithm, such as easy falling into local optimum, insufficient population diversity, and low convergence accuracy. In view of the above shortcomings, this paper introduced an improved multi-objective honey badger algorithm to solve the MOPRO problem based on sine chaotic mapping strategy, backward learning mechanism, and cross-learning mechanism. For all I know, the original algorithm and the proposed method in this paper are applied for the first time in the MORPO problem. To validate the comprehensive ability of the proposed method, MOIHBA, MOPSO, NGSA-II, and MODE are tested in IEEE30, IEEE57, and IEEE118 standard test systems, respectively, the GD index and HV index are chosen as two multi-objective evaluation indexes to further evaluate the improved algorithm.

The remaining components of this paper are structured as follows. Section II mainly introduces the MORPO problem in detail. Section III focuses on the original honey badger algorithm (HBA) and gives the steps of three improvement strategies. Section IV is the algorithm's simulation experiment and the analysis of the evaluation indexes. The conclusion section is shown in Section V.

II. MATHEMATICAL MODEL OF MORPO

The general representation of multi-objective reactive power optimization aims to optimize the pre-defined system objectives by finding suitable control variables, optimizing the nonlinear fitness function, and realizing the conditions of equality constraints and inequality constraints of the system at the same time [29]. The mathematical model for MORPO problem consists of two main components: objective and constraint. The MORPO problem can be defined by the following formulas:

$$min \ F(x,u) = \{f_1(x,u), f_2(x,u)...f_n(x,u)\} \quad (1)$$

$$G_i(x,u) = 0, \qquad i = 1,2,...m_i \quad (2)$$

$$H_j(x,u) \le 0, \qquad j = 1,2,...m_j \quad (3)$$

where f_1, f_2, and f_n are different objective functions; n is the amount of objective functions; $G_i(x,u)$ is expressed as the ith

equality constraint. $H_j(x,u)$ is expressed as the jth inequality constraint; m_i represents the number of equality constraints, m_j represents the number of inequality constraints.

$$x^T = [Q_{G_1}, Q_{G_2}, ...Q_{G_{N_V}}, V_1, V_2, ...V_{N_Q}, S_{L_1}, S_{L_2}, ...S_{L_{N_E}}] \quad (4)$$

where x^T stands for the state variable vector, Q_G represents the reactive power output at the PV node, N_V represents the total amount of PV nodes; V represents the voltage at the PQ node, N_Q indicates the number of PQ nodes; S_L indicates the apparent power on a branch, N_E represents the total number of branches.

$$u^T = [V_{G_1}, V_{G_2}, ...V_{G_{N_V}}, T_1, T_2, ...T_{N_T}, Q_{C_1}, Q_{C_2}, ...Q_{C_{N_C}}] \quad (5)$$

where u^T represents the vector of control variables, V_G represents the terminal voltage constraint of the generator; T represents the constraint of transformer tap ratio, N_T indicates the number of transformers; Q_C indicates the reactive power output constraint of the reactive power compensation device, and N_C represents the number of reactive power compensation devices.

A. Objective Functions

1) Active power losses minimization

Minimizing active power loss is the primary objective of reactive power optimization problem research, and it is also an important index to assess the economy of the power grid. The formula of its objective function is as follows:

$$f_1 = \min P_{loss} = \min[\sum_{k=1}^{N_i} g_k(V_i^2 + V_j^2 - 2V_iV_j \cos\theta_{ij})] \quad (6)$$

where V_i is the voltage magnitude at bus i; V_j represents the voltage magnitude at bus j; N_i indicates the number of buses; g_k indicates conductance; θ_{ij} indicates the voltage phase angle.

2) Voltage stability index

In solving the MORPO problem, the voltage stability index is also taken into account. The voltage stability index is defined as maintaining the voltage amplitude at each load bus within an acceptable range under rated conditions. Improving voltage stability can be achieved by minimizing a voltage stability criterion called *Lindex* at each network bus [30]. Its objective function is defined as follows:

$$f_2 = \min f_{Lindex} = \min(Lindex) = \max(L_j), \quad j \in N_Q \quad (7)$$

$$L_j = \left|1 - \sum_{i=1}^{N_V} K_{ji} \frac{V_i}{V_j}\right| \quad (8)$$

$$K_{ji} = -[Y_1]^{-1}[Y_2] \quad (9)$$

where f_{Lindex} represents the objective function of the voltage stability indicator; The symbol *Lindex* indicates the whole system voltage stability indicator; L_j is an indicator of local voltage stability; N_V indicates the number of PV nodes; V_i and V_j denote the complex voltage at the ith PV node as well as the jth PQ node respectively; Y_1 and Y_2 are sub-matrix of the grid derivative matrix determined by separating the PQ and PV node parameters.

3) Voltage deviation minimization

In power systems, voltage is one of the most significant parameters for measuring power quality, and in addition to the economics of the grid, the stability of the power grid also needs to be considered. Therefore, in the MORPO problem, voltage deviation should also be considered as one objective besides the above two objectives. Thus, this function is

presented as follows:

$$f_3 = minf_{Vd} = min\left\{\sum_{i=1}^{N_Q}|V_i - V_{REF}|\right\} \qquad (10)$$

where f_{Vd} stands for the objective function of the voltage deviation; N_Q represents the total amount of PQ nodes. V_i indicates the voltage at PQ node; V_{REF} denotes the ideal voltage with a per-unit value of 1.

B. Problem Constraints

In a MORPO problem, all objective functions are bounded by constraints. All constraints should be kept within their acceptable physical limits. These constraints are divided into two categories, one with equation constraints and the other with inequality constraints.

1) Equality constraints

The equality constraint equation is also called the power flow constraint equation [31]. This equation needs to satisfy the active and reactive power balance. The equality constraint equation is as follows:

$$P_{Gi} - P_{Li} - V_i \sum_{j \in N_i} V_j \left(g_{ij}\cos\theta_{ij} + b_{ij}\sin\theta_{ij}\right) = 0, \ \ i \in N \quad (11)$$

$$Q_{Gi} - Q_{Li} - V_i \sum_{j \in N_i} V_j \left(g_{ij}\cos\theta_{ij} - b_{ij}\sin\theta_{ij}\right) = 0, \ \ i \in N_P \quad (12)$$

where P_{Gi} and Q_{Gi} indicate the active and reactive power injected at the ith node; P_{Li}, Q_{Li} represents the active and reactive power consumed by the load at the ith node; V_i, V_j indicate the voltage magnitude at nodes i, j respectively; g_{ij} represents the conductance between nodes i, j; b_{ij} represents the susceptance between nodes i and j; N_i represents the number of nodes connected between node i and node j.

2) Inequality constraints

According to different types of variables, inequality constraints can be divided into two categories [32]. One is the state variable inequality constraint, and the other is the control variable inequality constraint.

a)State variable inequality constraints

When solving the MORPO problem, the state variables need to be controlled within the allowed range, such as the voltage at the PQ node, the reactive power output at the PV node, and the apparent power of the branch.

1: Voltage constraints at PQ nodes

$$V_i^{min} \le V_i \le V_i^{max}, \ \ i \in N_Q \qquad (13)$$

2: Reactive power constraints at PV nodes

$$Q_{Gi}^{min} \le Q_{Gi} \le Q_{Gi}^{max}, \ \ i \in N_V \qquad (14)$$

3: Branch apparent power constraint

$$S_{Li} \le S_{Li}^{max}, \ \ i \in N_E \qquad (15)$$

b)Control variable inequality constraints

To guarantee the reliability and sustainability of the electrical system, the voltage of each generator in the system, the transformer tap ratio, and the reactive power output of the reactive power compensator are all constrained [33].

1: Terminal voltage constraint of generator

$$V_{Gi}^{min} \le V_{Gi} \le V_{Gi}^{max}, \ \ i \in N_V \qquad (16)$$

2: Tap ratio constraint of transformer

$$T_i^{min} \le T_i \le T_i^{max}, \ \ i \in N_T \qquad (17)$$

3: Reactive power output limitation of reactive power compensator

$$Q_{Ci}^{min} \le Q_{Ci} \le Q_{Ci}^{max}, \ \ i \in N_C \qquad (18)$$

C. Multi-objective Constraint Processing Strategy

When solving the MORPO problem, the processing of constraints is a significant point. It will affect the result of algorithm optimization whether the constraints are handled well or not.

1) Handling strategies for constraint

For equality constraints, the power flow calculation can be used to verify whether the equality constraints meet the conditions. For the inequality constraints of control variables, it will be dealt with as follows:

$$u_k = \begin{cases} u_{k(min)} & if \ \ u_k < u_{k(min)} \\ u_k & if \ \ u_{k(min)} < u_k < u_{k(max)} \\ u_{k(max)} & if \ \ u_{k(max)} < u_k \end{cases} \qquad (19)$$

The state variable is generated by the power flow calculation. For the constraint processing of the state variable, the traditional method is to add the penalty coefficient method. This method has two disadvantages. One is that different penalty coefficient values should be adopted in different scenes. Secondly, in the same scene, it is difficult to determine the appropriate penalty coefficient value, and its too large or too small value will affect the optimization result. In this paper, a constraint-dominant hierarchical mechanism is proposed for the constraint processing of state variables. The concrete steps are listed below.

Step 1: Record the state variables that violate the constraints after the power flow calculation. If the state variable violates the constraints, the total constraints of the individual are calculated according to (20). The formula is shown below:

$$T\_vio(u_i) = \sum_{j=1}^{m_j} \max(0, H_j(x, u_i)) \qquad (20)$$

where, $T\_vio(u_i)$ represents the total number of individual violation of constraints, and m_j represents the number of inequality constraints.

Step 2: Comparing the sum of any two individuals' violation of constraints, there will be three situations.

1: Individual i dominates individual j.

$$T\_vio(u_i) < T\_vio(u_j) \qquad (21)$$

2: Individual j dominates individual i.

$$T\_vio(u_i) > T\_vio(u_j) \qquad (22)$$

3: When any two individuals violate the same total constraint values, the objective function values are compared:

$$\begin{cases} \forall \ k \in \{1,2,...n\} \ \ f_k(x, u_i) \le f_k(x, u_j) \\ \exists \ l \in \{1,2,...n\} \ \ f_l(x, u_i) < f_l(x, u_j) \end{cases} \qquad (23)$$

where, for any k belonging to 1 to n, $f_k(x,u_i)$ is not greater than $f_k(x,u_j)$, and there is at least one l that makes $f_l(x,u_i)$ less than $f_l(x,u_j)$, and l belongs to 1 to n. Thereby, individual i pareto dominates individual j.

2) Multi-objective sorting methods

A fast non-dominant sorting method with an elite strategy is used in this paper to obtain the POS [33]. This method calculates individuals' rank and crowding distance for stratification and ranking.

a)Hierarchical ranking of non-inferior solutions

Hierarchical ranking of non-inferior solutions is the process of dividing the solution set into different levels of pareto front. The specific steps are listed below:

Step 1: Assign two parameters, $N(i)$ and $S(i)$, to each solution in the population. $N(i)$ represents the total amount of individuals that dominate individual i in the population, and $S(i)$ represents the set of solutions dominated by individual i.

Step 2: Locate all individuals in the population for which $N(i)=0$, that is, all individuals i in the group that are not dominated by other individuals, and store these individuals in the set $F(1)$, and record the total number of the set as j, and record their rank as $Rank_0$. $Rank_0$ is the initial level, and is set to 1.

Step 3: For each individual l in $F(1)$, find out the set dominated by individual l, namely $S(l)$, and subtract 1 from the $N(l)$ corresponding to each individual l in the set $S(l)$, that is, the number of dominating individual l minus 1. And let its rank be $Rank=Rank_0+1$.

Step 4: Then repeat the above steps, and record the ranking of each individual until all individuals are stored in a certain set $F(i)$.

b)Crowding distance

When two individuals have different levels, the individual with the smaller $Rank$ value is selected. If two individuals are in the same hierarchy, to facilitate sorting, a crowding distance operator is introduced for sorting. For two individuals with the same $Rank$ value, calculate the crowding distance of the individuals, sort them by crowding distance at the same level from largest to smallest, and select solution with the larger crowding distance first. The process of execution is as follows:

Step 1: Select the kth target, calculate the distance between individual i and its adjacent individuals on the target, that is, the difference between the target values of individual $i+1$ and individual $i-1$, and finally, normalize the value.

Step 2: Traverse all objectives and add the normalized crowding distance values for each objective. The crowding distance formula is defined by the following equations:

$$cd(i) = \sum_{k=1}^{M} cd_k(i)$$
$$cd_k(i) = \frac{f_k(i+1) - f_k(i-1)}{f_k^{\max} - f_k^{\min}} \tag{24}$$

where $cd_k(i)$ represents the crowding distance of the ith individual. M represents the number of objective functions in MORPO. $fmax$ and $fmin$ represent the lowest and highest values of the kth objective function respectively.

c)Best compromise solution

After optimization of the algorithm, the obtained Pareto optimal sets are mutually exclusive. The previous processing method is to assign weight coefficients to different objective functions, and artificially judge which objective is more important. However, the disadvantage of this method is that it is difficult to find a suitable weight coefficient, and it is difficult to say which objective value is more important in some engineering applications, therefore, the conventional methods often produce suboptimal solutions. This paper adopts fuzzy theory to choose the best compromise solution (BCS) [34], and we consider the BCS as the most appropriate solution. The implementation process is as follows:

Step 1: In the pareto optimal set, find out the maximum value $\max[f_k(i)]$ and the minimum value $\min[f_k(i)]$ of the kth objective function.

Step 2: Calculate the fuzzy membership degree $Fm_k(i)$ of the kth objective function of the ith solution. The elementary procedures are as follows:

1: When the target value $f_k(i)$ is less than or equal to $\min[f_k(i)]$, $Fm_k(i)=1$;

2: When the target value $f_k(i)$ is greater than or equal to $\max[f_k(i)]$, $Fm_k(i)=0$;

3: When the target value $f_k(i)$ belongs to the interval $(\min[f_k(i)], \max[f_k(i)])$;

$$Fm_k(i) = \frac{\max[f_k(i)] - f_k(i)}{\max[f_k(i)] - \min[f_k(i)]} \tag{25}$$

Step 3: Combined with all objectives and calculate the satisfaction value $st(i)$ for each solution. The formula is as follows:

$$st(i) = \frac{\sum_{k=1}^{M} Fm_k(i)}{\sum_{i=1}^{n}\sum_{k=1}^{M} Fm_k(i)} \tag{26}$$

Step 4: Find the solution corresponding to the maximum satisfaction value $\max[st(i)]$, and select this solution as the best compromise solution.

III. RESEARCH ON HBA FOR MORPO PROBLEM

The initial honey badger algorithm is characterized by fewer parameters, better searchability and faster convergence, and this algorithm is used for the first time in the field of MORPO problem. However, this algorithm still has some disadvantages, such as poor search ability, inadequate initial population diversity, and low convergence accuracy. For this reason, three different improvements have been proposed for this algorithm.

A. The Basic Honey Badger Algorithm

The HBA is a new group intelligence optimization algorithm proposed by Fatma A. Hashim in 2021, which is inspired by honey badger predation. The optimization strategy of HBA is divided into two stages, one is the exploration stage, and the other is the exploitation stage, which can also be defined as global optimization stage and local optimization stage, respectively. The HBA can choose to execute the global search process or the local search process through a random number. The mathematical formula for the global search phase is as follows ($rand<0.5$):

$$x_{new} = x_{prey} + F \times \beta \times I \times x_{prey} + F \times r_1 \times a \times d_i \times A \tag{27}$$

$$A = |\cos(2 \times \pi \times r_2) \times [1 - \cos(2 \times \pi \times r_3)]| \tag{28}$$

where x_{new} stands for the updated positio; x_{prey} stands for the global optimal position and β indicates the potential of the honey badger to obtain food with a value greater than or equal to 1. I_i stands for the odor intensity of the prey, if the value is large, the speed will be fast; d_i represents the distance between the current honey badger individual and x_{prey}, the detailed formula is as follows.

$$I_i = r_4 \times \left(\frac{(x_i - x_{i+1})^2}{4 \times (\pi \times d_i^2)}\right) \tag{29}$$

$$d_i = x_{prey} - x_i \tag{30}$$

In the above formulas, F represents the function that alters the search direction; a represents the density factor, which is used to ensure the smooth shift of the algorithm from global to local search. The formula is as follows:

$$F = \begin{cases} 1 & if \ (rand \le 0.5) \\ -1 & otherwise \end{cases} \tag{31}$$

$$a = C \times \exp(\frac{-t}{t_{\max}}) \tag{32}$$

The mathematical formula of the local search stage is as follows ($rand$>0.5):

$$x_{new} = x_{prey} + F \times r_5 \times a \times d_i \tag{33}$$

where r_1, r_2, r_3, r_4 and r_5 represent the random numbers between 0 and 1. $rand$ is also a random number between 0 and 1.

B. Proposed MOIHBA

1) Sine chaotic mapping strategy

In the HBA algorithm, the initialization of the population is randomly distributed. This method is likely to cause the location of the population to be concentrated in a certain feasible region, so the algorithm has poor diversity and ergodicity in the early search, which further affects the algorithm's search accuracy and convergence speed [35]. The sine chaotic model is a chaotic model with infinite number of mapping folds, which has good ergodicity and randomness. Therefore, this method will be used to improve the diversity of the population. Its expression is as follows:

$$\begin{cases} R_{i+1} = \sin(\frac{2}{R_i}) & i = 0,1,...,N \\ -1 \le R_i \le 1 & R_i \ne 0 \end{cases} \tag{34}$$

$$X_{i+1} = R_{i+1} \times (ub - lb) + lb \tag{35}$$

where R_i is a random number between -1 and 1, and it is not 0; X_{i+1} represents the position of the individual; ub, lb represent the maximum and minimum position constraint limits.

2) Backward learning mechanism

After adopting the sine chaotic mapping strategy, the ergodicity and diversity of the population are improved, but the problem is that in the process of algorithm optimization, the search range of the solution set is too large, and the optimization time is too long. In response to this problem, a backward learning mechanism will be introduced, which can improve the quality of the solution set of the initial population and narrow the search range. After the generated population is initialized, its reverse population is calculated, the fitness of the initial population and the reverse population is merged, and the calculation results are sorted non-inferiorly. Finally, the top individuals are taken as the initial population. It can be described as below:

$$converseX_i = ub + lb - X_i \tag{36}$$

where X_i represents the position of the initial individual; $converseX_i$ represents the reverse position of the initial individual. ub and lb represent the maximum and minimum position constraint limits.

3) Cross-learning mechanism

As the optimization accuracy of the original HBA algorithm is not high, a cross-learning mechanism will be introduced. The selection intersection strategy of DE algorithm can better enable the algorithm to traverse the entire search domain so that it is easier to find potential optimal solutions. Therefore, in order to improve the optimization accuracy of HBA and expand the diversity of the population, the crossover process of the DE algorithm is

introduced into the mining stage of the honey badger algorithm (The global search stage). Its mathematical form is defined as follows:

$$F(i) = f_{R1}(i) + \eta \times (f_{R2}(i) - f_{R3}(i))$$
$$R1、R2、R3 \in [1，N] \tag{37}$$

where $F(i)$ represents the newly generated individuals after crossover, $R1$, $R2$, and $R3$ represent three random numbers with different values between 1 and N, respectively; η represents the step size operator which is used to control the degree of individual variation. $f_{R1}(i)$, $f_{R2}(i)$ and $f_{R3}(i)$ respectively represent three different individuals from the population. The specific crossover process is as follows:

$$\begin{cases} X_i = F(i) & if \ R_c \le VC \\ X_i = X_i & else \end{cases} \tag{38}$$

where X_i represents the individual position; R_c represents a random number; VC represents a cross constant, which is 0.3. The pseudo-code of MOIHBA is as follows.

TABLE I
PSEUDO-CODE OF MOIHBA

Start
Set initial values for variables like N, D, β, C, t_{max}, VC, η.
Generate the initial population using (34,35,36).
Count the target and constraint values for each individual and rank the $2N$ individuals;
Take the first N individuals;
Select the best individual as x_{prey} and record it fitness value to f_{prey};
t=0;
while $t < t_{max}$
    Update the factor α using (32);
  for $i = 1 \ to \ N$
    Calculate the intensity I_i using (29);
    Generate a vector $F(i)$ using (37);
    for $j=1 \ to \ D$
      if $rand$<0.5
        Execute the crossover strategy for X_i according to (38);
        Update the position X_{new} using (27) (global search);
      else
        Update the position X_{new} using (33) (local search);
      end
    end
  end
  Obtain a new population and record each fitness value;
  if $f_{new} \le f_i$
  $X_i = X_{new}$ and $f_i = f_{new;}$;
  end
  if $f_{new} \le f_{prey}$
  Select the best individual as x_{prey} and record it fitness value to f_{prey};
  end
  t=t+1;
end while

IV. SIMULATION RESULTS AND COMPARISONS

To test the effectiveness and practicability of MOIHBA, nine multi-objective cases were tested under three different sized test systems, they are IEEE30, IEEE57, and IEEE118, while MOPSO/NSGA-II and MODE are chosen as the comparison algorithms. The simulation experiments are completed on a PC with i5-7500 CPU @ 3.40GHz with 16G memory. To further describe the MOIHBA algorithm, the detailed process is shown in IJg. 1.

A. Test Systems

The IEEE30 standard test system is shown in Fig. 2, and the specific data parameters of the system are shown in literature [36-38]. This test system has 19 control variables, including six generator variables, four transformer variables and nine reactive power compensator variables. In this

system, the upper limit of the generator bus voltage is set to 1.1 (p.u), and the lower limit is 0.95 (p.u). Transformer taps have an upper limit of 1.1 (p.u) and a lower limit of 0.9 (p.u).

The IEEE57 standard test system is shown in Fig. 3, and the specific data parameters of the system can be found in literature [39]. The vector of control variables in this system is a 27-dimensional vector, including 7 generators, 17 transformers and 3 reactive power compensation devices. Set the upper limit of the generator bus voltage to 1.1 (p.u) and

the lower limit to 0.9 (p.u). Transformer taps have an upper limit of 1.1 (p.u) and a lower limit of 0.9 (p.u).

The IEEE118 standard test system is shown in Fig. 4, and the detailed data parameters of this system are presented in literature [39]. This test system is larger and more complex than the IEEE30 and IEEE57 test systems. The system has 75 control variables, including 54 generators variables, 9 transformers variables, and 12 reactive power compensator variables.
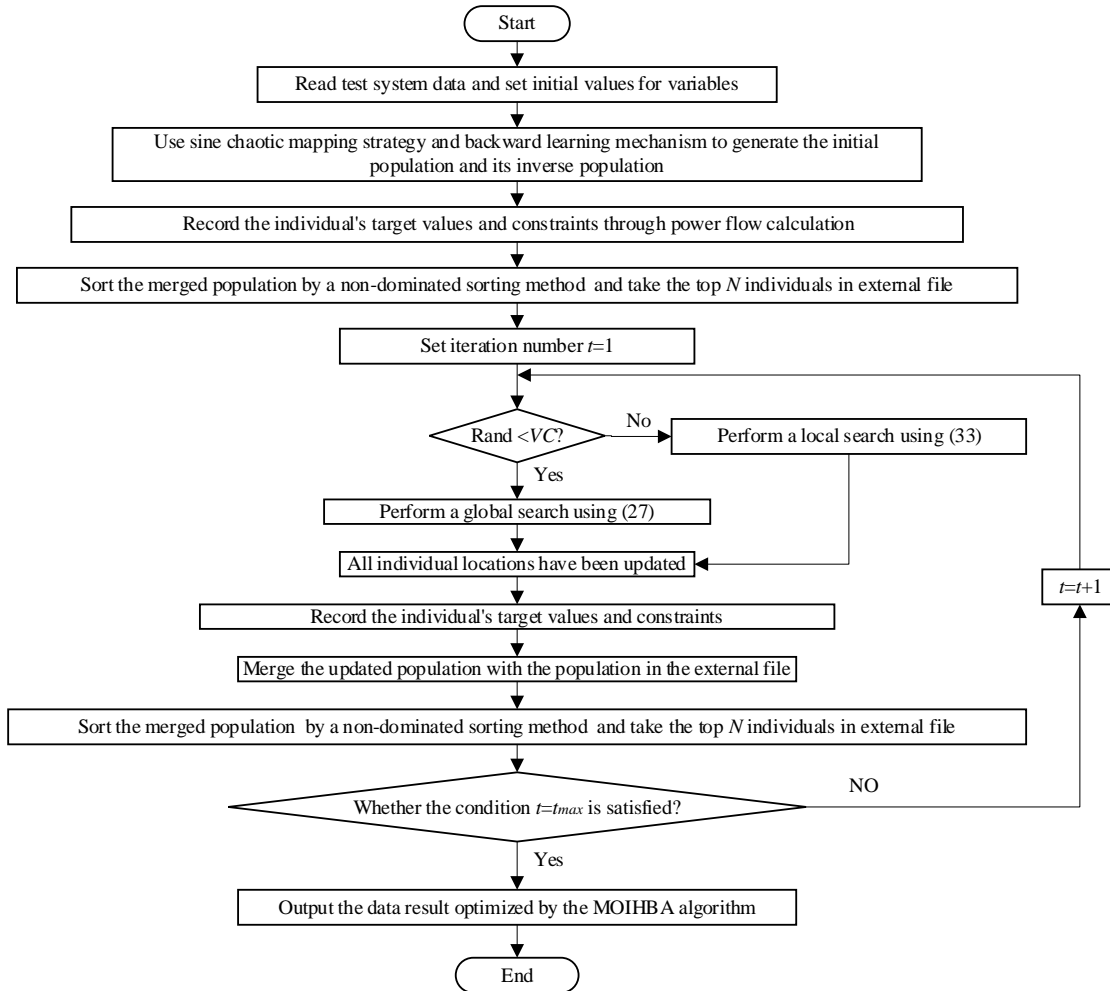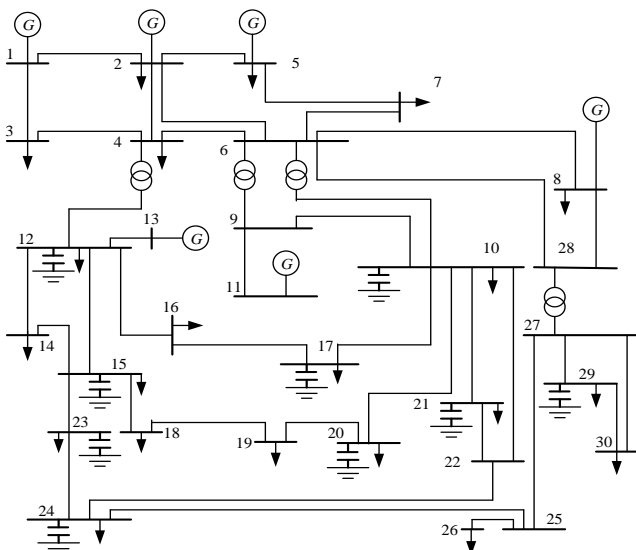

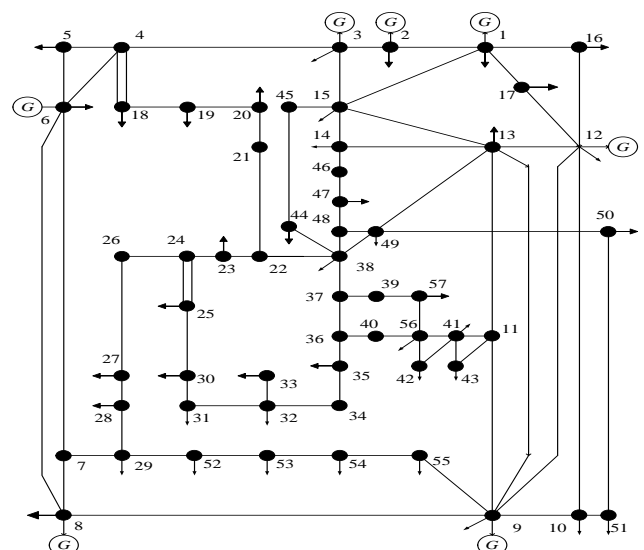Fig. 1. The flow chart of MORPO method

Fig. 2. IEEE30 standard test system

Fig. 3. IEEE57 standard test system

B. Algorithm Parameters Settings

Setting the appropriate parameters of the algorithm is a very important step. To determine the magnitude of the population and the total amount of iterations of MOIHBA algorithm, experiments will be conducted on the IEEE30 standard test system for a two-objective mathematical model consisting of f_{Ploss} and f_{Lindex}.

When the population size is 100, and the number of iterations is from 50 to 400, the simulation results in Fig. 5. The best PFs are obtained when the number of iterations is 300 and 400, in order to shorten the experiment time, the number of iterations is set to 300. When setting the population size to 30, 60, 100 and 150 and the number of iterations to 300, from Fig. 6, it is clear that the optimal PFs are gained when the population size is 100 and 150. By comprehensive consideration, the initial group size N is set to 100. TABLE II sets specific values for the variables of the MOIHBA algorithm. Apart from the specific parameters mentioned in the table, the detailed parameter settings of MOPSO and NSGA-II are described in references [38] and [36]. Set the variable F to 0.5 and CR to 0.3 in the MODE algorithm. In the following experiments, the reference capacity is set to 100MVA.
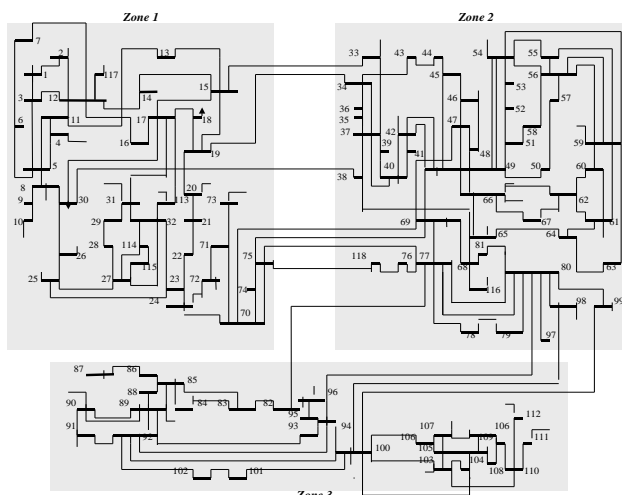

Fig. 4. IEEE118 standard test system
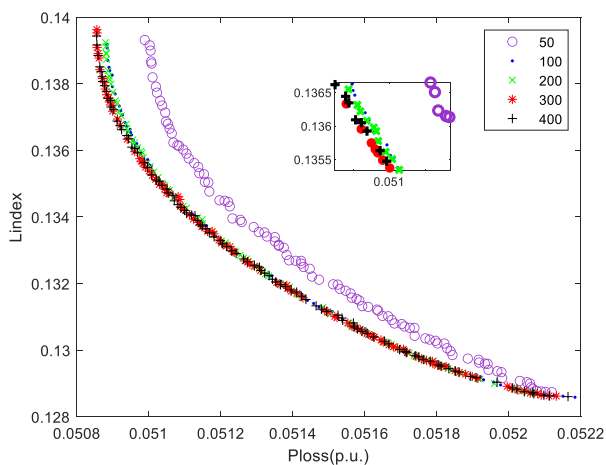
Fig. 5. Pareto fronts in different iterations

C. IEEE30 Standard Test System

1) Case 1

In this case, two main objective functions are optimized. It

clearly shows the PFs obtained by three different algorithms in Fig. 7, and the pareto front of MOIHBA is closer to the real solution. Fig. 8 shows the location of the BCS of MOIHBA. TABLE III gives the optimization results of several algorithms' BCS. TABLE IV demonstrated the comparative data of the best compromise solutions obtained by several algorithms, which is solved by using a fuzzy theory method. The active power loss value of MOIHBA is 5.1202 MW, and the voltage stability index is 0.1332, and the results are better than MOPSO and NSGA-II. When comparing with reference [15], although the voltage stability index of MOIHBA is slightly higher than that of MOCIPSO, the active power loss value is significantly lower than that of MOCIPSO,

Fig. 6. Pareto fronts in different populations

Fig. 7. PFs obtained by three algorithms in Case 1

Fig. 8. The BCS of MOIHBA in Case 1

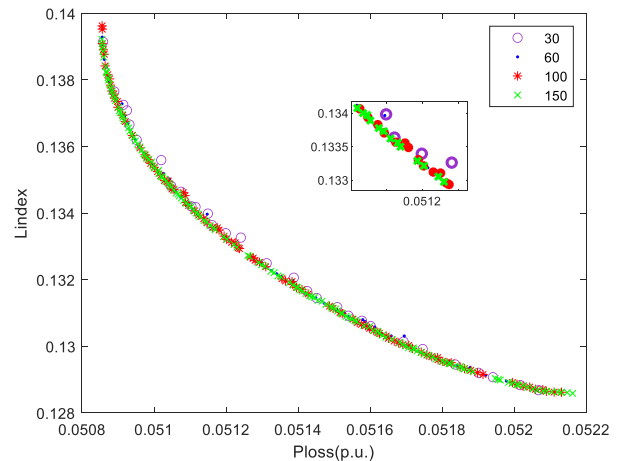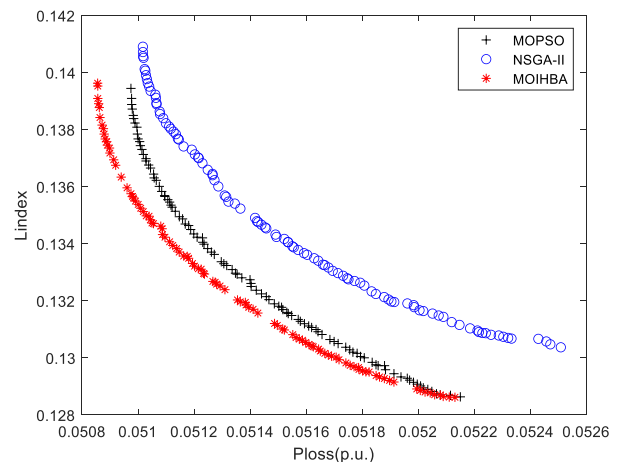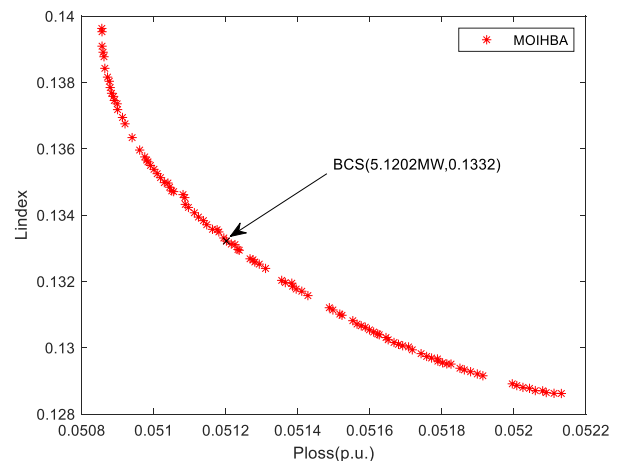which indicates that the proposed MOIHBA can solve the MORPO problem well and the introduced strategies have been effectively incorporated in original algorithm.

2) Case 2

The active power losses and voltage deviation are optimized in this case. Fig. 9 demonstrates the PFs obtained by MOIHBA algorithm, MOPSO algorithm, and NSGA-II algorithm, and it can be observed that the pareto front of MOIHBA are better. Fig. 10 shows the location of the best compromise solution of MOIHBA. TABLE V lists the values of the adjusted control variables for obtaining the best compromise through several algorithms. TABLE VI displays the comparison of the best compromise solutions acquired by several algorithms and references [40]. The active power loss of MOIHBA is 5.1368 MW, and the voltage deviation is 0.2471. By comparing with several other algorithms and references, obviously, it demonstrates that the MOIHBA algorithm outperforms several other algorithms, and it shows the effectiveness and competitiveness of the proposed method.

<div align="center">

TABLE II
PARAMETER SETTING OF MOIHBA ALGORITHM

</div>

Algorithms	Parameters	Case1~9
	Population	100
	Maximum Iteration	300
	External file size	100
MOIHBA	C	2
	β	6
	VC	0.3
	η	0.5

<div align="center">

TABLE III
BCS OPTIMIZATION RESULTS IN CASE 1

</div>

Control variables	MOPSO	NSGA-II	MOIHBA
V_{G1}(p.u.)	1.1000	1.1000	1.0315
V_{G2}(p.u.)	1.0077	0.9517	1.0972
V_{G5}(p.u.)	1.1000	0.9755	1.0999
V_{G8}(p.u.)	1.1000	1.0038	1.0987
V_{G11}(p.u.)	1.1000	1.0151	1.1000
V_{G13}(p.u.)	0.9500	0.9664	0.9906
T_{6-9}	0.9784	0.9690	0.9827
T_{6-10}	0.9000	0.9239	0.9000
T_{4-12}	0.9419	0.9689	0.9443
T_{28-27}	0.9260	0.9166	0.9166
C_{10}(p.u.)	0.0500	0.0346	0.0500
C_{12}(p.u.)	0.0500	0.0392	0.0500
C_{15}(p.u.)	0.0500	0.0446	0.0500
C_{17}(p.u.)	0.0500	0.0480	0.0500
C_{20}(p.u.)	0.0500	0.0402	0.0500
C_{21}(p.u.)	0.0500	0.0408	0.0500
C_{23}(p.u.)	0.0399	0.0479	0.0423
C_{24}(p.u.)	0.0500	0.0445	0.0500
C_{29}(p.u.)	0.0500	0.0279	0.0287
f_{Ploss}(MW)	5.1297	5.1494	**5.1202**
$f_{L\,index}$	0.1334	0.1342	**0.1332**

<div align="center">

TABLE IV
COMPARISON OF BEST COMPROMISE SOLUTIONS IN CASE 1

</div>

comparison	f_{Ploss}(MW)	$f_{L\,index}$
MOIHBA	**5.1202**	**0.1332**
MOPSO	5.1297	0.1334
NSGA-II	5.1494	0.1342
MOCIPSO[38]	5.2320	0.1182

3) Case 3

In order to make the system operate stably in the MORPO problem, the two single objectives of voltage stability index and voltage deviation are combined into a double objective

mathematical model. As can be seen in Fig. 11, although the PFs of the three algorithms are similar, the distributivity and uniformity of the pareto front of MOIHBA are somewhat preferable over the other algorithms. Fig. 12 gives the location of the BCS of MOIHBA. TABLE VII and TABLE VIII summarize the BCS obtained by several algorithms, and the BCS of MOIHBA includes voltage deviation and voltage stability index, which are 0.4117 and 0.1343, respectively. The comparison shows that MOIHBA is preferable to several other algorithms. Although the numerical gap in the obtained optimization data is not significant, considering the large scale of the test system, the optimization advantage of MOIHBA cannot be ignored.
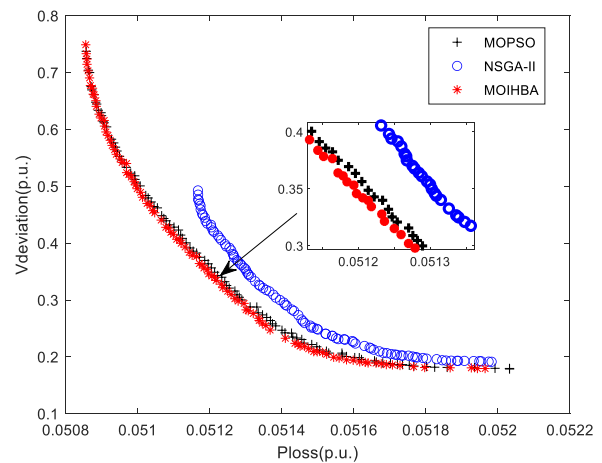
Fig. 9. PFs obtained by three algorithms in Case 2
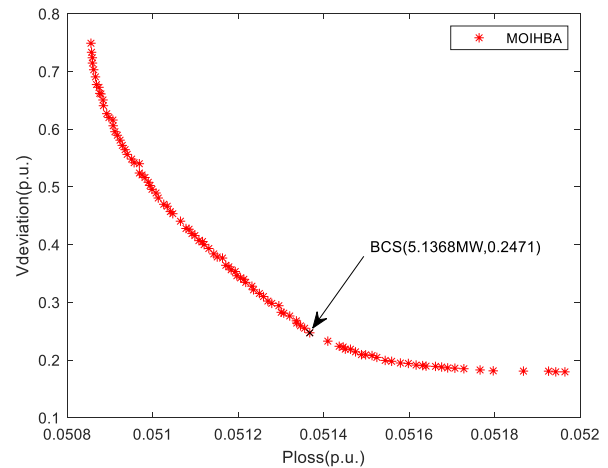
Fig. 10. The BCS of MOIHBA in Case 2

D. IEEE57 Standard Test System

4) Case 4

The optimization of active power loss and voltage stability index within IEEE57 standard test system is a further test for the proposed algorithm. As can be seen in Fig. 13, the distributivity and uniformity of the PFs obtained by several algorithms are slightly inferior to those of case 1, which may be due to the increase in the scale of the test system. However, the PF of MOIHBA is better than MOPSO and MODE according to the picture display. Fig. 14 shows the location of the BCS of MOIHBA. TABLE IX and TABLE X show the optimization results of BCS and the comparison with references. As can be seen that the BCS of MOIHBA includes the active power loss and voltage stability indexes, which are

TABLE V
BCS OPTIMIZATION RESULTS IN CASE 2

Control variables	MOPSO	NSGA-II	MOIHBA
V_{G1}(p.u.)	1.1000	1.0595	1.0785
V_{G2}(p.u.)	1.0687	0.9862	1.0904
V_{G5}(p.u.)	1.0974	1.0871	1.0928
V_{G8}(p.u.)	1.1000	0.9608	1.0931
V_{G11}(p.u.)	1.0236	1.0776	0.9587
V_{G13}(p.u.)	1.1000	1.0019	1.0983
T_{6-9}	1.0776	1.0780	1.0755
T_{6-10}	0.9000	0.9008	0.9001
T_{4-12}	1.0260	1.0214	1.0248
T_{28-27}	0.9789	0.9748	0.9774
C_{10}(p.u.)	0	0.0412	0.0024
C_{12}(p.u.)	0	0.0018	0.0008
C_{15}(p.u.)	0.0500	0.0255	0.0363
C_{17}(p.u.)	0.0500	0.0470	0.0489
C_{20}(p.u.)	0.0500	0.0351	0.0390
C_{21}(p.u.)	0.0500	0.0253	0.0500
C_{23}(p.u.)	0.0196	0.0321	0.0272
C_{24}(p.u.)	0.0500	0.0475	0.0500
C_{29}(p.u.)	0.0219	0.0246	0.0222
f_{Ploss}(MW)	5.1374	5.1482	**5.1368**
f_{V_d} (p.u.)	0.2581	0.2516	**0.2471**

TABLE VI
COMPARISON OF BEST COMPROMISE SOLUTIONS IN CASE 2

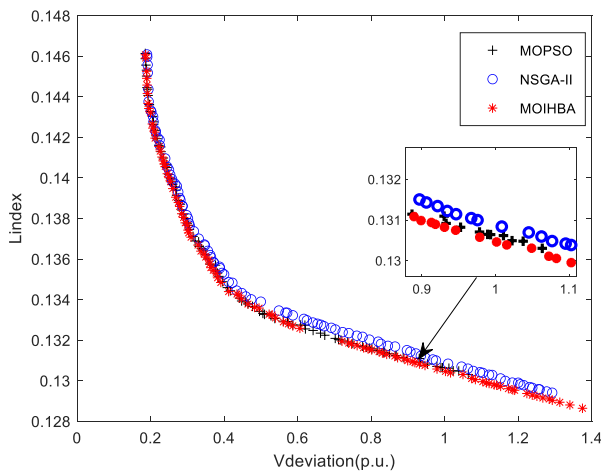| comparison	f_{Ploss}(MW)	f_{V_d} (p.u.)
MOIHBA	**5.1368**	**0.2471**
MOPSO	5.1374	0.2581
NSGA-II	5.1482	0.2516
MOICA[40]	5.1483	0.2623
MOGBICA[40]	5.1383	0.2483

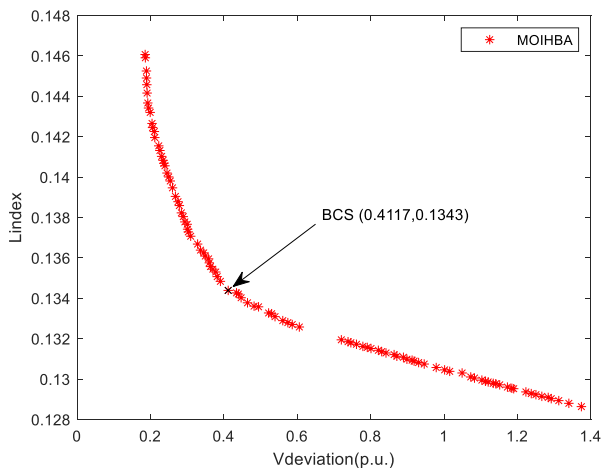Fig. 11. PFs obtained by three algorithms in Case 3

Fig. 12. The BCS of MOIHBA in Case 3

26.7923 MW and 0.2639, respectively, with better performance compared with other algorithms. In comparison with references, the active power losses are significantly lower than in MOCIPSO, although the voltage stability index is not as good as in MOCIPSO.

TABLE VII
BCS OPTIMIZATION RESULTS IN CASE 3

Control variables	MOPSO	NSGA-II	MOIHBA
V_{G1}(p.u.)	1.0926	0.9722	1.0200
V_{G2}(p.u.)	1.0862	0.9520	1.0137
V_{G5}(p.u.)	1.1000	1.0936	1.0773
V_{G8}(p.u.)	1.1000	1.0338	1.0542
V_{G11}(p.u.)	1.1000	0.9500	1.0864
V_{G13}(p.u.)	1.0071	1.0969	0.9880
T_{6-9}	1.1000	1.0169	1.0730
T_{6-10}	0.9000	0.9661	0.9000
T_{4-12}	1.1000	1.0676	1.0783
T_{28-27}	0.9000	0.9004	0.9000
C_{10}(p.u.)	0.0500	0.0174	0
C_{12}(p.u.)	0.0277	0.0143	0
C_{15}(p.u.)	0.0500	0.0220	0.0500
C_{17}(p.u.)	0.0026	0.0247	0
C_{20}(p.u.)	0.0500	0.0485	0.0500
C_{21}(p.u.)	0.0361	0.0129	0.0130
C_{23}(p.u.)	0.0258	0.0107	0.0179
C_{24}(p.u.)	0	0.0265	0.0270
C_{29}(p.u.)	0.0500	0.0499	0.0500
f_{V_d} (p.u.)	0.4165	0.4335	**0.4117**
$f_{L\,index}$	0.1344	0.1345	**0.1343**

TABLE VIII
COMPARISON OF BEST COMPROMISE SOLUTIONS IN CASE 3

comparison	f_{V_d} (p.u.)	$f_{L\,index}$
MOIHBA	**0.4117**	**0.1343**
MOPSO	0.4165	0.1344
NSGA-II	0.4335	0.1345

5) Case 5

In case 5, the selection of the objective function is the same as in case2. Fig. 15 demonstrates the pareto front of MOIHBA outperforms than MOPSO and MODE. Fig. 16 clearly shows the location of the BCS for MOIHBA. TABLE XI shows the optimal control variables for several algorithms to obtain the best compromise solution. From TABLE XII, it can be seen that the BCS of MOIHBA is 26.9287 (MW), 1.1586 (p.u.), and its values are significantly better than MOPSO and MODE, respectively. Therefore, it can be further verified that MOIHBA can perform well in medium-sized test systems.
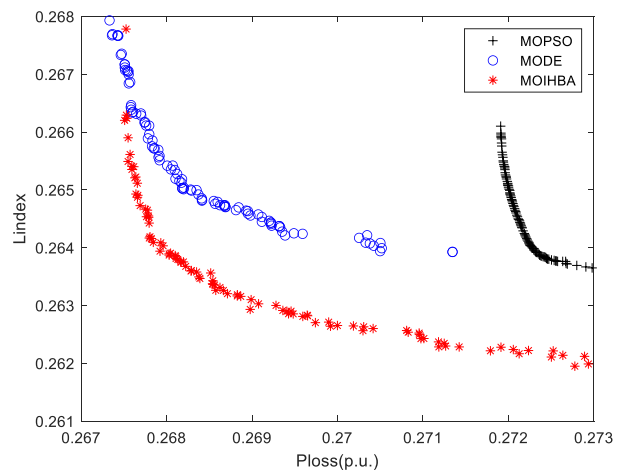

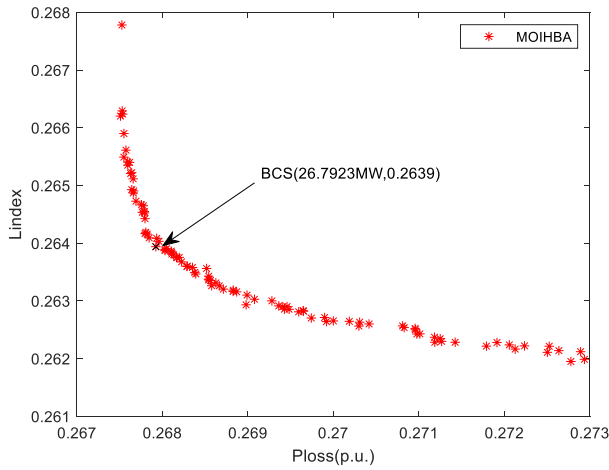Fig. 13. PFs obtained by three algorithms in Case 4
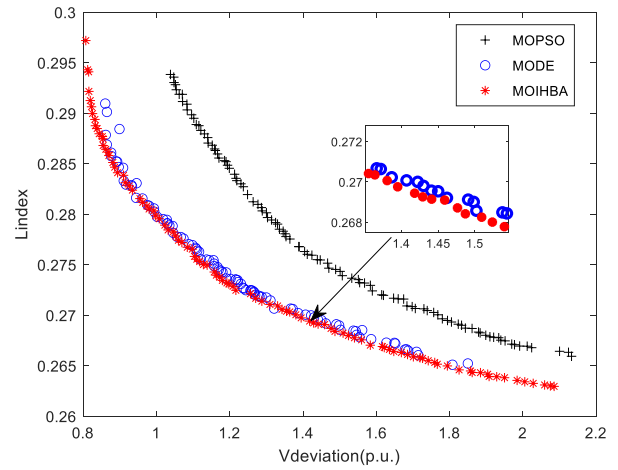
Fig. 14. The BCS of MOIHBA in Case 4

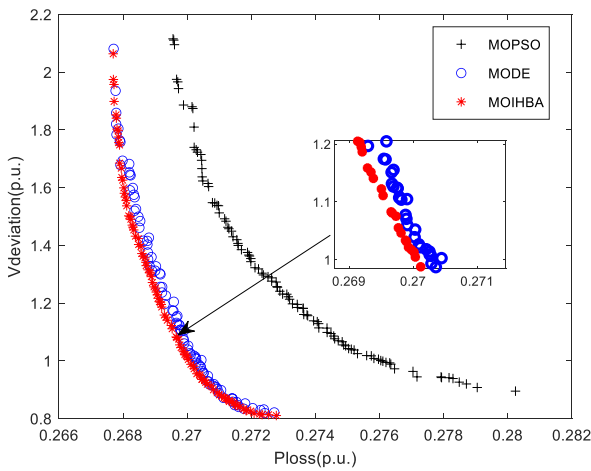Fig. 17. PFs obtained by three algorithms in Case 6

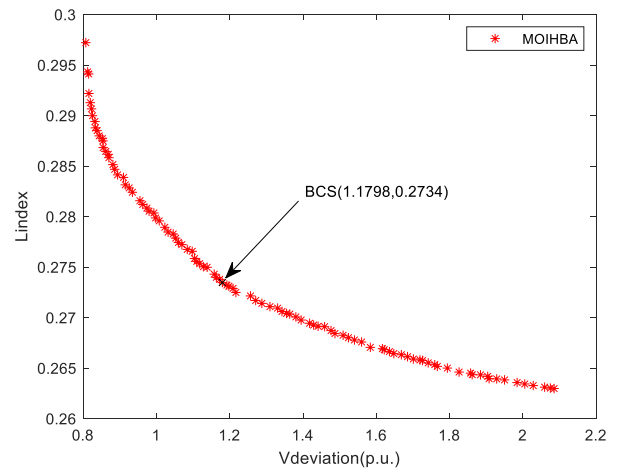Fig. 15. PFs obtained by three algorithms in Case 5

Fig. 18. The BCS of MOIHBA in Case 6
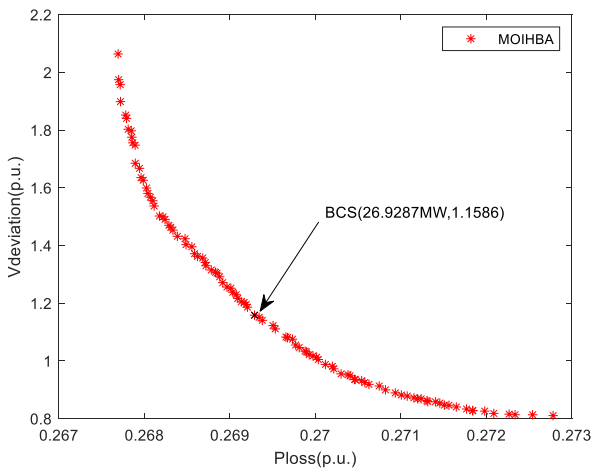
Fig. 16. The BCS of MOIHBA in Case 5

6) Case 6

In case 6, MOIHBA, MOPSO, and MODE are used for the optimization of the voltage deviation and voltage stability index, and from Fig. 17, it can be seen clearly that the distribution and uniformity of the pareto front obtained by MOIHBA are better and closer to the true front than MOPSO and MODE. Fig. 18 shows the BCS location of MOIHBA. From TABLE XIII and TABLE XIV, it can be seen that the values of BCS of MOIHBA are 1.1798 (p.u.) and 0.2734, respectively. This data set reflects that MOIHBA is superior to MOPSO and MODE.

TABLE IX
BCS OPTIMIZATION RESULTS IN CASE 4

Control variables	MOPSO	MODE	MOIHBA
V_{G1}(p.u.)	1.1000	1.1000	0.9005
V_{G2}(p.u.)	0.9000	1.0878	0.9074
V_{G3}(p.u.)	0.9000	1.0061	0.9274
V_{G6}(p.u.)	0.9000	0.9623	0.9270
V_{G8}(p.u.)	0.9000	1.1000	0.9200
V_{G9}(p.u.)	1.1000	0.9579	1.0081
V_{G12}(p.u.)	1.1000	0.9297	0.9491
$T_{4\text{-}18}$	0.9000	0.9011	0.9043
$T_{4\text{-}18}$	0.9000	0.9030	0.9065
$T_{21\text{-}20}$	1.0386	1.0036	1.0043
$T_{24\text{-}25}$	0.9000	1.0114	0.9530
$T_{24\text{-}25}$	0..9000	0.9204	0.9756
$T_{24\text{-}26}$	1.0176	1.0041	0.9941
$T_{7\text{-}29}$	0.9000	0.9163	0.9000
$T_{34\text{-}32}$	0.9000	0.9000	0.9004
$T_{11\text{-}41}$	0.9000	0.9002	0.9014
$T_{15\text{-}45}$	0.9000	0.9000	0.9001
$T_{14\text{-}46}$	0.9000	0.9000	0.9003
$T_{10\text{-}51}$	0.9000	0.9000	0.9000
$T_{13\text{-}49}$	0.9000	0.9001	0.9001
$T_{11\text{-}43}$	0.9000	0.9001	0.9008
$T_{40\text{-}56}$	1.0794	1.0611	1.0666
$T_{39\text{-}57}$	0.9000	1.0162	1.0230
$T_{9\text{-}55}$	0.9000	0.9038	0.9006
C_{18}(p.u.)	0	0.1372	0.1243
C_{25}(p.u.)	0	0.0902	0.0853
C_{53}(p.u.)	0.1097	0.1199	0.0956
f_{Ploss}(MW)	27.2249	26.8182	**26.7923**
$f_{L\,\text{index}}$	0.2641	0.2650	**0.2639**

TABLE X
COMPARISON OF BEST COMPROMISE SOLUTIONS IN CASE 4

comparison	f_{Ploss}(MW)	$f_{L\,index}$
MOIHBA	**26.7923**	**0.2639**
MOPSO	27.2249	0.2641
MODE	26.8182	0.2650
MOCIPSO[38]	27.1220	0.2370

E. IEEE118 Standard Test System

7) Case 7

IEEE118 is a much larger scale standard test system, which is used in this case to verify MOIHBA, MOPSO, MODE, and NSGA-II for the dual objective of active power loss and voltage deviation combination. In Fig. 19, the PFs of the four algorithms can be obtained, and it can be clearly seen that the pareto front of the MOIHBA algorithm outperforms the other three algorithms. The position of the BCS of MOIHBA is given in Fig. 20. TABLE XV obtains the values of the adjusted control variables for each algorithm.

TABLE XVI gives the values of the BCS of MOIHBA, which are 131.6729 (MW) and 1.2774 (p.u.), and their values are better than the other three algorithms and MOICA-III [41]. This reflects that the performance of MOIHBA when applied to large-scale test systems is competitive and efficient.

TABLE XI
BCS OPTIMIZATION RESULTS IN CASE 5

Control variables	MOPSO	MODE	MOIHBA
V_{G1}(p.u.)	1.1000	1.0137	0.9889
V_{G2}(p.u.)	1.1000	1.0250	1.0694
V_{G3}(p.u.)	1.1000	0.9411	0.9727
V_{G6}(p.u.)	1.0829	1.0400	0.9440
V_{G8}(p.u.)	0.9207	1.0128	0.9639
V_{G9}(p.u.)	1.1000	1.0048	1.0738
V_{G12}(p.u.)	1.1000	0.9273	1.0916
T_{4-18}	0.9781	0.9393	0.9583
T_{4-18}	0.9000	0.9871	0.9155
T_{21-20}	1.0260	1.0275	1.0185
T_{24-25}	0.9000	0.9406	0.9432
T_{24-25}	1.1000	1.0760	1.0740
T_{24-26}	1.0225	1.0064	1.0089
T_{7-29}	0.9512	0.9324	0.9359
T_{34-32}	0.9000	0.9599	0.9613
T_{11-41}	0.9000	0.9065	0.9057
T_{15-45}	0.9000	0.9242	0.9187
T_{14-46}	0.9000	0.9194	0.9204
T_{10-51}	0.9340	0.9304	0.9335
T_{13-49}	0.9000	0.9000	0.9010
T_{11-43}	0.9000	0.9054	0.9059
T_{40-56}	1.1000	1.0371	1.0095
T_{39-57}	0.9000	0.9674	0.9721
T_{9-55}	0.9455	0.9227	0.9239
C_{18}(p.u.)	0	0.1243	0.0502
C_{25}(p.u.)	0.0979	0.1315	0.1301
C_{53}(p.u.)	0.1178	0.1107	0.1041
f_{Ploss}(MW)	27.2115	26.9294	**26.9287**
f_{Vd} (p.u.)	1.3227	1.1968	**1.1586**

TABLE XII
COMPARISON OF BEST COMPROMISE SOLUTIONS IN CASE 5

comparison	f_{Ploss}(MW)	f_{Vd} (p.u.)
MOIHBA	**26.9287**	**1.1586**
MOPSO	27.2115	1.3227
MODE	26.9294	1.1968

8) Case 8

In case 8, the voltage deviation and voltage stability index are selected as the optimization objectives. The pareto fronts of the three algorithms are given in Fig. 21, and by processing

the graphs, it can be observed that the pareto front obtained by the MOIHBA algorithm is better than the other two algorithms, and Fig. 22 shows the location of the BCS for MOIHBA. TABLE XVII displays the values of the control variables optimized by each algorithm. The data of the BCS of MOIHBA are given in TABLE XVIII, which are 1.3032 (p.u.) and 0.0671. Compared with the other two algorithms, the comprehensive performance of the proposed algorithm is more competitive. All the above cases fully verify that the proposed algorithm perform well as well as practical in test systems of different sizes.

TABLE XIII
BCS OPTIMIZATION RESULTS IN CASE 6

Control variables	MOPSO	MODE	MOIHBA
V_{G1}(p.u.)	1.0595	1.1000	1.0118
V_{G2}(p.u.)	1.0116	0.9000	0.9790
V_{G3}(p.u.)	1.1000	1.1000	0.9731
V_{G6}(p.u.)	0.9000	1.0606	1.0454
V_{G8}(p.u.)	0.9000	0.9000	1.0022
V_{G9}(p.u.)	0.9552	0.9000	0.9582
V_{G12}(p.u.)	0.9000	0.9685	0.9327
T_{4-18}	1.1000	0.9624	0.9220
T_{4-18}	0.9000	1.0415	1.0936
T_{21-20}	0.9556	1.0074	0.9839
T_{24-25}	0.9000	0.9000	0.9000
T_{24-25}	1.1000	0.9000	0.9006
T_{24-26}	1.0186	1.0109	1.0052
T_{7-29}	0.9548	0.9516	0.9270
T_{34-32}	0.9000	0.9000	0.9038
T_{11-41}	0.9000	0.9005	0.9004
T_{15-45}	0.9000	0.9000	0.9034
T_{14-46}	0.9000	0.9000	0.9074
T_{10-51}	0.9000	0.9948	0.9914
T_{13-49}	0.9329	0.9055	0.9009
T_{11-43}	0.9418	0.9004	0.9106
T_{40-56}	1.0635	1.0800	1.0359
T_{39-57}	0.9000	0.9220	0.9422
T_{9-55}	0.9000	0.9433	0.9489
C_{18}(p.u.)	0	0.2533	0.2202
C_{25}(p.u.)	0.1623	0.0495	0.0494
C_{53}(p.u.)	0	0.0678	0.0111
f_{Vd} (p.u.)	1.4116	1.1903	**1.1798**
$f_{L\,index}$	0.2761	0.2737	**0.2734**

TABLE XIV
COMPARISON OF BEST COMPROMISE SOLUTIONS IN CASE 6

comparison	f_{Vd} (p.u.)	$f_{L\,index}$
MOIHBA	**1.1798**	**0.2734**
MOPSO	1.4116	0.2761
MODE	1.1903	0.2737

9) Case 9

Compared with the double-objective optimization problem, the optimization of three objectives simultaneously requires the higher performance of the algorithm. In case 9, to verify the proposed algorithm is also effective in solving the three-objective optimization problem in MORPO, three conflicting goal functions, namely, active power loss, voltage stability index and voltage deviation, will be optimized at the same time. Fig. 23 shows the PF distribution of MOPSO, MODE and MOIHBA algorithms. The diagram clearly shows the MOIHBA has a more uniform solution set, a wider range of solutions, and a better Pareto front than the other two algorithms. Fig. 24 shows the PF of MOIHBA. TABLE XIX shows the best compromise solutions obtained by three algorithms through fuzzy theory strategy. It shows the optimization results that the solution of

Fig. 19. PFs obtained by four algorithms in Case 7

Fig. 20. The BCS of MOIHBA in Case 7

TABLE XV
BCS Optimization Results in Case 7
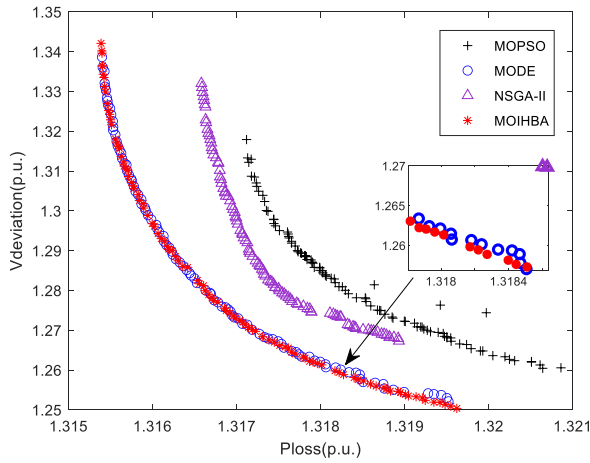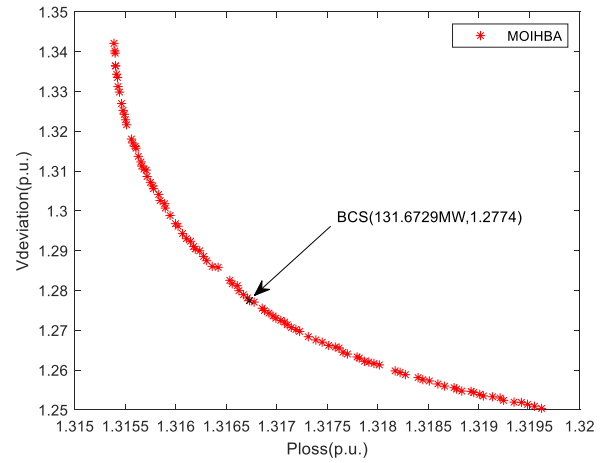
CVs	Alg1	Alg2	Alg3	Alg4	CVs	Alg1	Alg2	Alg3	Alg4
V_{G1}(p.u.)	0	0.9415	1.0477	0.9378	V_{G87}(p.u.)	0.9000	1.0572	0.9533	1.0032
V_{G4}(p.u.)	1.1000	1.0242	0.9878	0.9756	V_{G89}(p.u.)	0.9000	0.9341	1.0555	0.9692
V_{G6}(p.u.)	0.9000	1.1000	0.9000	0.9529	V_{G90}(p.u.)	0.9000	0.9000	0.9984	0.9415
V_{G8}(p.u.)	1.1000	0.9780	0.9053	0.9795	V_{G91}(p.u.)	1.1000	1.0870	0.9293	1.0228
V_{G10}(p.u.)	0.9000	0.9591	0.9170	0.9628	V_{G92}(p.u.)	0.9014	0.9000	1.0547	0.9509
V_{G12}(p.u.)	1.1000	0.9000	0.9542	0.9570	V_{G99}(p.u.)	1.1000	0.9169	0.9713	1.0078
V_{G15}(p.u.)	0.9000	0.9452	0.9227	0.9592	V_{G100}(p.u.)	0.9679	1.1000	1.0381	1.0345
V_{G18}(p.u.)	1.1000	0.9256	1.0442	0.9411	V_{G103}(p.u.)	0.9000	1.0497	1.0973	0.9403
V_{G19}(p.u.)	0.9000	1.0525	0.9924	0.9207	V_{G104}(p.u.)	0.9901	1.0245	1.0621	1.0517
V_{G24}(p.u.)	1.1000	1.0336	0.9409	0.9723	V_{G105}(p.u.)	0.9000	1.1000	1.0953	0.9821
V_{G25}(p.u.)	1.1000	0.9210	1.0069	0.9172	V_{G107}(p.u.)	0.9000	0.9317	1.0975	0.9615
V_{G26}(p.u.)	0.9000	1.0652	1.0905	1.0201	V_{G110}(p.u.)	1.1000	0.9953	1.0246	1.0532
V_{G27}(p.u.)	1.1000	1.0622	0.9082	0.9115	V_{G111}(p.u.)	1.1000	1.1000	0.9022	1.0421
V_{G31}(p.u.)	1.1000	1.0079	0.9152	0.9577	V_{G112}(p.u.)	0.9000	0.9063	0.9370	0.9668
V_{G32}(p.u.)	0.9176	0.9700	0.9028	1.0306	V_{G113}(p.u.)	0.9000	1.0153	1.0942	1.0058
V_{G34}(p.u.)	0.9755	0.9259	1.0432	0.9417	V_{G116}(p.u.)	0.9000	1.1000	0.9797	0.9204
V_{G36}(p.u.)	1.0951	0.9000	1.0715	0.9896	T_8	0.9944	0.9957	0.9971	0.9949
V_{G40}(p.u.)	0.9000	1.1000	0.9105	1.0201	T_{32}	0.9869	0.9907	0.9721	0.9904
V_{G42}(p.u.)	0.9444	1.0492	0.9708	0.9862	T_{36}	0.9950	1.0022	0.9864	1.0001
V_{G46}(p.u.)	1.1000	1.1000	0.9403	1.0407	T_{51}	0.9970	0.9955	1.0251	0.9959
V_{G49}(p.u.)	0.9272	0.9000	0.9757	0.9926	T_{93}	1.0124	1.0126	1.0232	1.0091
V_{G54}(p.u.)	0.9545	1.0001	1.0013	0.9618	T_{95}	0.9997	1.0042	0.9882	1.0081
V_{G55}(p.u.)	0.9005	0.9503	0.9206	1.0038	T_{102}	0.9710	0.9926	0.9854	0.9913
V_{G56}(p.u.)	1.0259	0.9733	1.0249	1.0568	T_{107}	0	0.9142	0.9409	0.0117
V_{G59}(p.u.)	0.9000	0.9628	1.0836	0.9925	T_{127}	0.9476	0.9448	0.9422	0.0464
V_{G61}(p.u.)	0.9000	0.9131	0.9650	1.0294	C_{34}(p.u.)	0	0	0.0233	0.0547
V_{G62}(p.u.)	0.9000	0.9549	0.9580	1.0582	C_{44}(p.u.)	0.3000	0.1427	0.1312	0.1492
V_{G65}(p.u.)	1.0254	0.9508	0.9011	0.9335	C_{45}(p.u.)	0	0.2552	0.2857	0.2475
V_{G66}(p.u.)	0.9695	1.0858	1.0219	0.9441	C_{46}(p.u.)	0	0.1655	0.1700	0.1318
V_{G69}(p.u.)	1.1000	0.9000	0.9045	0.9473	C_{48}(p.u.)	0	0.0325	0.0358	0.0231
V_{G70}(p.u.)	0.9000	0.9000	1.0004	1.0066	C_{74}(p.u.)	0	0.3000	0.2811	0.1555
V_{G72}(p.u.)	1.1000	1.0607	1.1000	1.0217	C_{79}(p.u.)	0.2282	0.3000	0.0466	0.2725
V_{G73}(p.u.)	0.9000	1.0405	0.9202	0.9102	C_{82}(p.u.)	0.3000	0.2998	0.1742	0.2949
V_{G74}(p.u.)	1.1000	1.0355	0.9661	0.9313	C_{83}(p.u.)	0.3000	0.3000	0.1110	0.2936
V_{G76}(p.u.)	0.9013	0.9104	0.9002	0.9801	C_{105}(p.u.)	0.3000	0.1563	0.1186	0.1319
V_{G77}(p.u.)	0.9000	1.0221	0.9156	0.9478	C_{107}(p.u.)	0	0.2614	0.0200	0.1040
V_{G80}(p.u.)	1.1000	1.0522	1.0281	0.9424	C_{110}(p.u.)	0	0.0393	0.0536	0.1494
V_{G85}(p.u.)	1.1000	0.9011	0.9110	0.9246	f_{Ploss}(MW)	131.8330	131.6734	131.9208	**131.6729**
					f_{V_d} (p.u.)	1.2792	1.2775	1.3160	**1.2774**

Note: CVs represents control variables; Alg1-Alg4 represent MOPSO, MODE, NSGA-II, MOIHBA, respectively

TABLE XVI
Comparison of Best Compromise Solutions in Case 7

comparison	f_{Ploss}(MW)	f_{V_d} (p.u.)
MOIHBA	**131.6729**	**1.2774**
MOPSO	131.8330	1.2792
MODE	131.6734	1.2775
NSGA-II	131.9208	1.3160
MOICA-III[41]	131.7112	1.2732

MOIHBA is superior to MODE, and although the individual solutions of MOIHBA are inferior to MOPSO, the overall quality of all the solutions obtained by MOIHBA is the highest from the PF. It demonstrates that MOIHBA can also solve the three-objective optimization problem well.

F. Performance Evaluation

For the evaluation indexes of multi-objective optimization, commonly used evaluation indexes include generation distance index (GD), hypervolume index (HV), inversion generation distance (IGD), spacing and so on. In this paper, GD and HV are selected as evaluation indexes.
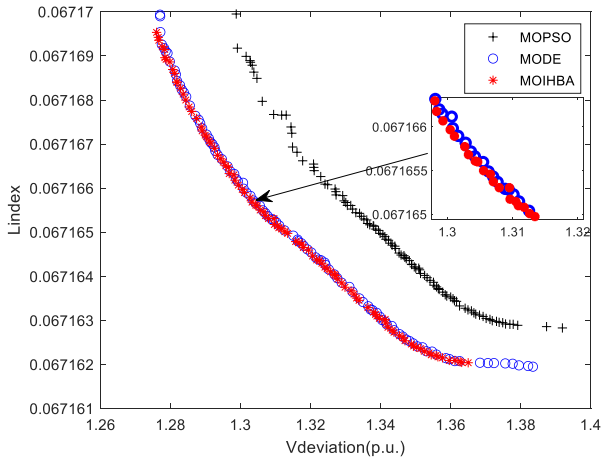
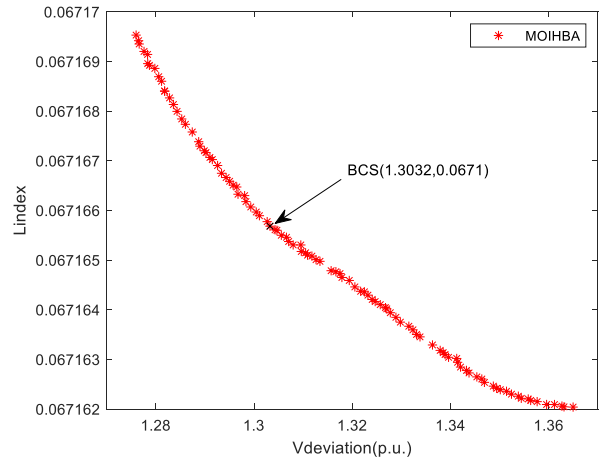Fig. 21. PFs obtained by three algorithms in Case 8

Fig. 22. The BCS of MOIHBA in Case 8

TABLE XVII
BCS OPTIMIZATION RESULTS IN CASE 8

CVs	Alg1	Alg2	Alg3	CVs	Alg1	Alg2	Alg3
V_{G1}(p.u.)	1.1000	1.0985	0.9708	V_{G87}(p.u.)	1.1000	1.0629	0.9000
V_{G4}(p.u.)	1.1000	1.0902	1.1000	V_{G89}(p.u.)	1.1000	1.0785	1.0378
V_{G6}(p.u.)	1.1000	1.0879	1.0396	V_{G90}(p.u.)	1.1000	1.0927	1.0395
V_{G8}(p.u.)	1.1000	1.0844	0.9853	V_{G91}(p.u.)	1.0243	1.0559	0.9572
V_{G10}(p.u.)	1.1000	1.0931	0.9228	V_{G92}(p.u.)	0.9000	1.1000	0.9752
V_{G12}(p.u.)	1.1000	1.0122	1.0247	V_{G99}(p.u.)	1.1000	1.0532	0.9142
V_{G15}(p.u.)	1.1000	1.0996	0.9060	V_{G100}(p.u.)	0.9000	1.0469	1.0528
V_{G18}(p.u.)	0.9000	0.9182	0.9547	V_{G103}(p.u.)	1.1000	1.0999	0.9000
V_{G19}(p.u.)	1.1000	1.0933	0.9000	V_{G104}(p.u.)	1.1000	1.0997	0.9506
V_{G24}(p.u.)	1.1000	1.0697	1.1000	V_{G105}(p.u.)	1.1000	1.0554	0.9000
V_{G25}(p.u.)	1.1000	1.0702	0.9319	V_{G107}(p.u.)	1.1000	1.0840	0.9000
V_{G26}(p.u.)	1.1000	1.0332	0.9000	V_{G110}(p.u.)	1.1000	1.0999	0.9000
V_{G27}(p.u.)	1.1000	1.0741	0.9000	V_{G111}(p.u.)	1.1000	1.0823	0.9848
V_{G31}(p.u.)	1.1000	1.0461	1.0446	V_{G112}(p.u.)	1.0880	0.9528	1.0343
V_{G32}(p.u.)	1.1000	0.9044	0.9861	V_{G113}(p.u.)	0.9598	0.9618	1.1000
V_{G34}(p.u.)	1.1000	1.0917	1.0524	V_{G116}(p.u.)	1.1000	1.0150	1.1000
V_{G36}(p.u.)	1.0128	1.0937	1.0141	T_8	0.9865	0.9935	0.9897
V_{G40}(p.u.)	1.1000	1.0104	0.9000	T_{32}	0.9900	0.9905	0.9903
V_{G42}(p.u.)	0.9000	0.9662	1.0837	T_{36}	1.0392	1.0388	1.0333
V_{G46}(p.u.)	1.1000	1.0416	0.9000	T_{51}	0.9792	0.9776	0.9837
V_{G49}(p.u.)	1.1000	0.9691	1.0649	T_{93}	1.0333	1.0232	1.0204
V_{G54}(p.u.)	1.1000	1.0111	1.0025	T_{95}	0.9765	0.9934	0.9946
V_{G55}(p.u.)	1.1000	1.0266	1.1000	T_{102}	0.9978	0.9954	1.0008
V_{G56}(p.u.)	1.1000	1.0952	1.1000	T_{107}	1.1000	0.9002	0.9005
V_{G59}(p.u.)	1.1000	1.0992	1.1000	T_{127}	0.9269	0.9467	0.9469
V_{G61}(p.u.)	1.1000	1.0661	0.9000	C_{34}(p.u.)	0	0.2454	0.1041
V_{G62}(p.u.)	1.1000	1.0739	0.9332	C_{44}(p.u.)	0.3000	0.3000	0.3000
V_{G65}(p.u.)	1.1000	1.0999	1.1000	C_{45}(p.u.)	0.3000	0.3000	0.3000
V_{G66}(p.u.)	1.1000	0.9550	0.9192	C_{46}(p.u.)	0.3000	0.2811	0.0238
V_{G69}(p.u.)	1.1000	0.9948	0.9651	C_{48}(p.u.)	0	0.0007	0.0010
V_{G70}(p.u.)	1.1000	1.0415	1.0805	C_{74}(p.u.)	0	0.0347	0.0639
V_{G72}(p.u.)	1.1000	0.9759	1.0454	C_{79}(p.u.)	0	0.0049	0.0002
V_{G73}(p.u.)	1.1000	0.9015	0.9000	C_{82}(p.u.)	0.3000	0.3000	0.3000
V_{G74}(p.u.)	1.1000	1.0910	1.0905	C_{83}(p.u.)	0.3000	0.2988	0.2989
V_{G76}(p.u.)	1.1000	1.0965	1.0074	C_{105}(p.u.)	0.3000	0.1958	0.1870
V_{G77}(p.u.)	1.1000	1.0542	0.9326	C_{107}(p.u.)	0.3000	0.2874	0.2989
V_{G80}(p.u.)	1.1000	0.9323	1.0139	C_{110}(p.u.)	0.3000	0.0177	0.3000
V_{G85}(p.u.)	1.1000	0.9776	1.0854	f_{V_d}(p.u.)	1.3272	1.3077	**1.3032**
				$f_{L\,index}$	0.0672	0.0672	**0.0671**

Note: CVs represents control variables; Alg1-Alg3 represent MOPSO, MODE, MOIHBA, respectively

TABLE XVIII
COMPARISON OF BEST COMPROMISE SOLUTIONS IN CASE 8

comparison	f_{V_d} (p.u.)	$f_{L\,index}$
MOIHBA	**1.3032**	**0.0671**
MOPSO	1.3272	0.0672
MODE	1.3077	0.0672

1) GD

In the multi-objective reactive power optimization problem, the GD index is used to evaluate the convergence performance of the pareto front obtained by the algorithm [42]. It mainly calculates the average separation from the algorithm's PF to its corresponding real PF. A smaller average distance proves a much more satisfactory convergence performance of the algorithm.

TABLE XIX
COMPARISON OF BEST COMPROMISE SOLUTIONS IN CASE 9

comparison	f_{Ploss}(MW)	$f_{L\,index}$	f_{V_d} (p.u.)
MOIHBA	**132.0725**	**0.0673**	**1.2835**
MOPSO	132.1261	0.0672	1.3137
MODE	132.2659	0.0674	1.2838

The specific formula is as follows:

$$GD = \frac{(\sum_{i=1}^{n} Ed_i^2)^{1/2}}{n} \qquad (39)$$

where n indicates the overall amount of non-inferior solutions, Ed_i indicates the Euclidean distance of the ith solution from real PF.

2) HV

The hypervolume index is adopted to measure the comprehensive performance of the algorithm, such as diversity, cutting-edge and convergence [11]. It mainly calculates the volume of the area enclosed between the PF obtained by the calculation algorithm and the reference point.

HV index represents the overall performance of the algorithm. The specific formula is as follows:

$$HV = \delta(\bigcup_{i=1}^{|n|} v_i) \qquad (40)$$

where δ indicates the Lebesgue measure for the volume. $|n|$ means the overall amount of non-dominated solutions. v_i indicates the hypervolume shaped by the ith solution and its reference point.

3) Statistical result analysis

Based on the previous eight case studies, two indexes, GD and HV are selected to investigate the performance of each algorithm, and the results will be presented in a box plot.

The main function of the box plot is to find the overall distribution within the data, including minimum, maximum,
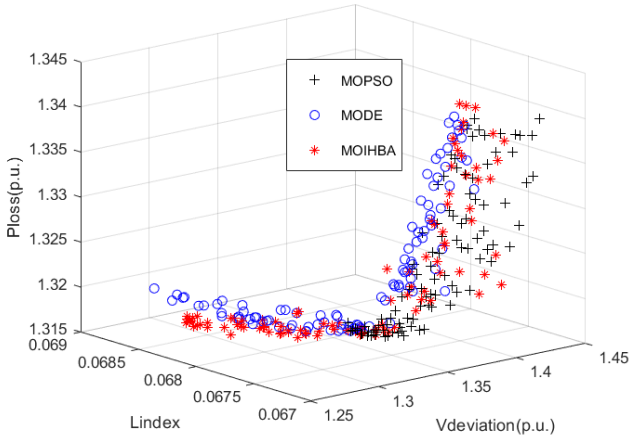

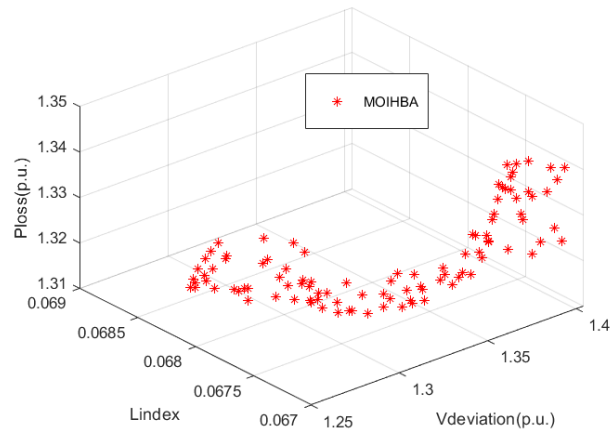Fig. 23. PFs obtained by three algorithms in Case 9
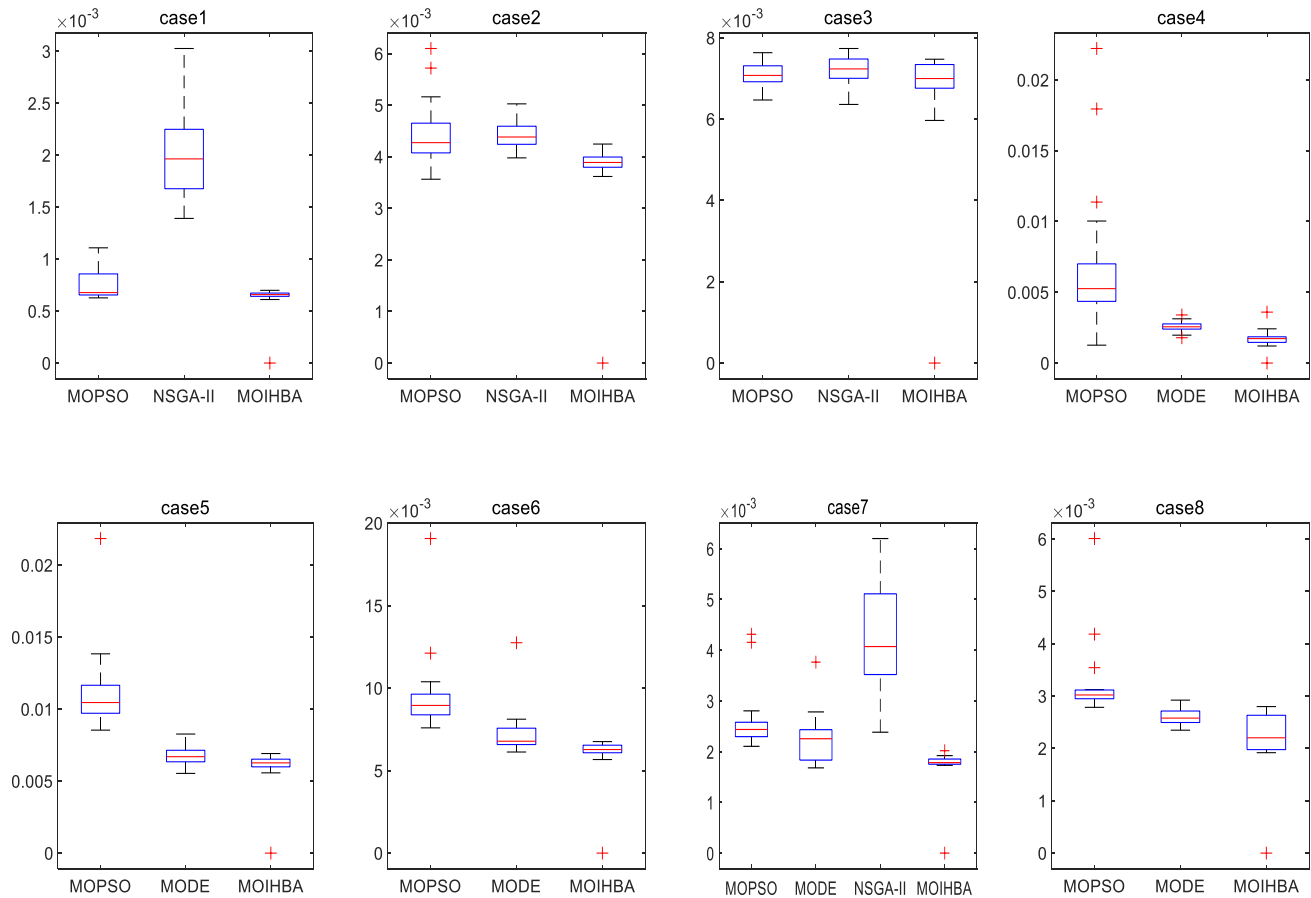

Fig. 24. The PF of MOIHBA in Case 9

Fig. 25. Boxplots of GD index for several algorithms
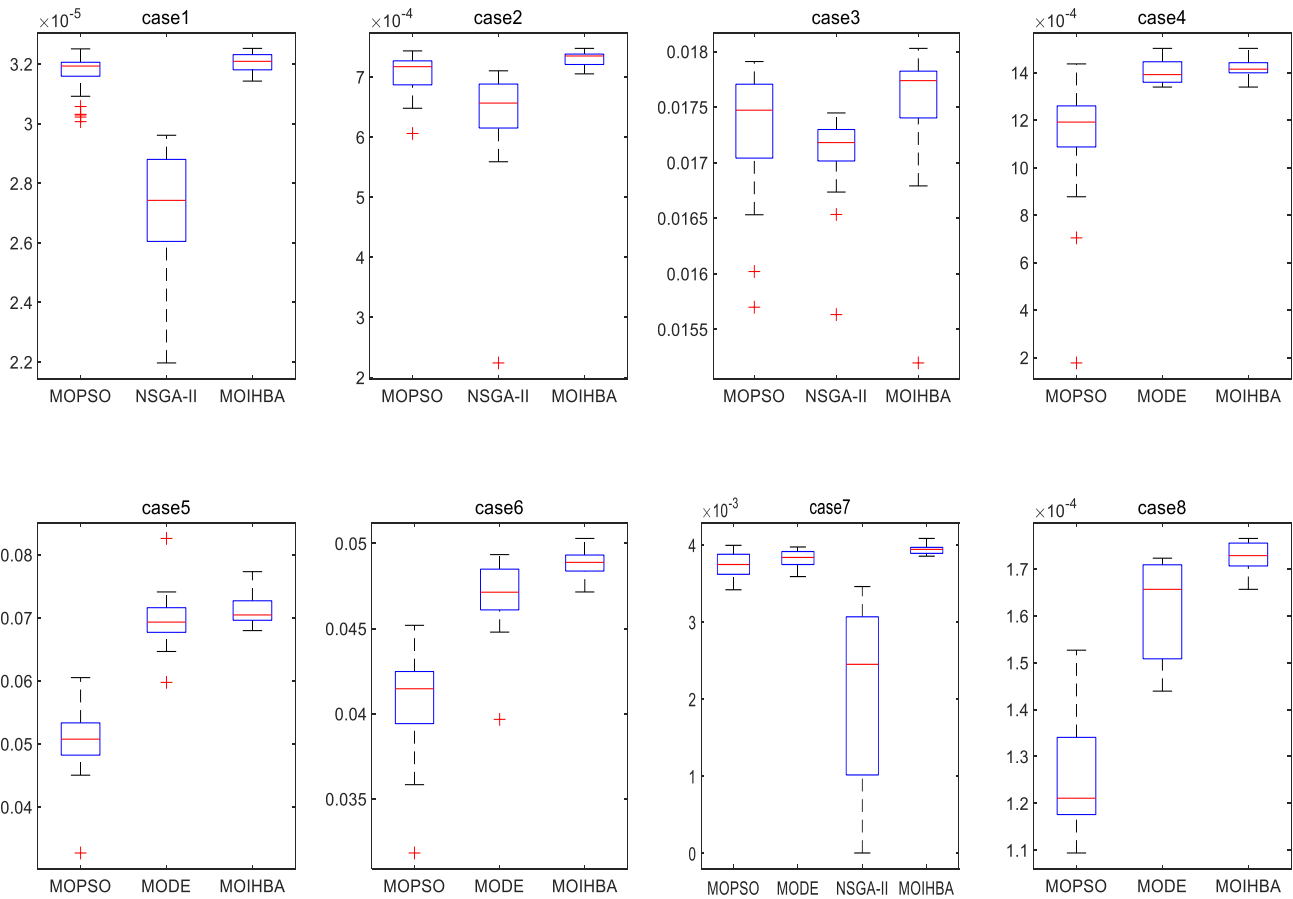
Fig. 26. Boxplots of HV index for several algorithms

TABLE XX
THE VALUES OF GD INDEXES FOR SEVERAL ALGORITHMS

Index	Cases	Type of data	MOIHBA	MOPSO	NSGA-II	MODE
	Case1	Mean	0.000636	0.000768	0.002002	-
		Deviation	0.000122	0.000158	0.000376	-
	Case2	Mean	0.003779	0.004431	0.004437	-
		Deviation	0.00073	0.000551	0.000251	-
	Case3	Mean	0.006763	0.007087	0.007207	-
		Deviation	0.001334	0.000254	0.000361	-
	Case4	Mean	0.001721	0.006464	-	0.002558
		Deviation	0.000648	0.004448	-	0.000339
GD	Case5	Mean	0.005944	0.010959	-	0.006782
		Deviation	0.001573	0.002412	-	0.000687
	Case6	Mean	0.006082	0.009359	-	0.007279
		Deviation	0.001157	0.002067	-	0.001408
	Case7	Mean	0.001722	0.002608	0.004295	0.002218
		Deviation	0.000411	0.000582	0.001116	0.000491
	Case8	Mean	0.002071	0.003234	-	0.002597
		Deviation	0.000839	0.000718	-	0.000174

TABLE XXI
THE VALUES OF HV INDEXES FOR SEVERAL ALGORITHMS

Index	Cases	Type of data	MOIHBA	MOPSO	NSGA-II	MODE
	Case1	Mean	0.000032	0.000032	0.000027	-
		Deviation	2.78665E-07	6.80144E-07	2.01075E-06	-
	Case2	Mean	0.000730	0.000700	0.000630	-
		Deviation	0.000011	0.000032	0.000091	-
	Case3	Mean	0.017675	0.017282	0.017093	-
		Deviation	0.000239	0.000542	0.000348	-
	Case4	Mean	0.001420	0.001110	-	0.001400
		Deviation	0.000042	0.000270	-	0.000050
HV	Case5	Mean	0.071297	0.050159	-	0.069725
		Deviation	0.002568	0.005912	-	0.004801
	Case6	Mean	0.048833	0.040677	-	0.046980
		Deviation	0.000910	0.003116	-	0.002176
	Case7	Mean	0.003940	0.003746	0.002045	0.003830
		Deviation	0.000060	0.000157	0.001173	0.000118
	Case8	Mean	0.000170	0.000130	-	0.000160
		Deviation	0.000004	0.000013	-	0.000011

TABLE XXII
THE AVERAGE RUNNING TIME FOR SEVERAL ALGORITHMS

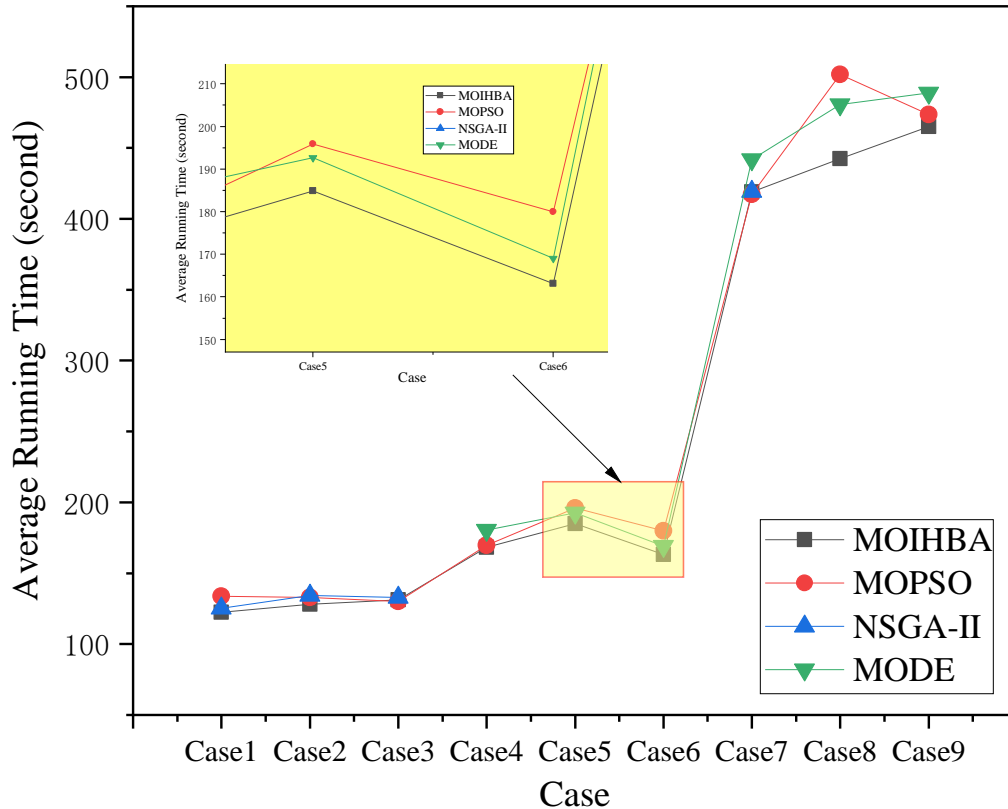| Algorithms	Cases								
	Case1	Case2	Case3	Case4	Case5	Case6	Case7	Case8	Case9
MOIHBA	122.4381	128.2116	131.2872	168.3002	184.9136	163.1296	418.8992	442.3404	465.1260
MOPSO	133.6267	132.9078	130.0905	169.6388	195.9156	179.9868	417.2444	501.8284	473.5467
NSGA-II	125.2728	134.4408	132.8664	–	–	–	419.1788	–	–
MODE	–	–	–	180.4910	192.7396	169.1127	441.9246	480.7238	488.9296

Fig. 27. Dot line graph of average running time for several algorithms

quantile, median and outlier values.

In Fig. 25, the GD values of eight cases are calculated respectively. A smaller value of GD in an algorithm indicates that the algorithm has better convergence performance. It can be seen from the eight box plots, the GD index of MOIHBA has the smallest fluctuation and a lower mean value. Therefore, the results suggest a better convergence performance and stability for proposed algorithm in solving the MORPO problem.

In Fig. 26, the HV values of each algorithm are analyzed in the same way. From the box plots, a higher mean value for MOIHBA compared to other algorithms can be clearly seen, in most cases, the fluctuation range of its value is smaller, and there is no outlier. This indicates that MOIHBA can obtain POS with better diversity. TABLE XX and TABLE XXI demonstrate the detailed numerical value of GD and HV obtained by each algorithm in each case. According to the data results, the value of MOIHBA is better in most cases.

The algorithm complexity can be used as an evaluation method to reflect the running effect of algorithms. The algorithm time complexity, that is, the average running time, is used for analysis in this study. TABLE XXII shows the average running time of MOIHBA and other comparison algorithms in each case. From these data, although the running time of MOIHBA algorithm is slightly longer than

other algorithms in individual cases, on the whole, MOIHBA algorithm takes less time to solve MORPO problems than other algorithms. From Fig. 27, a more intuitive view can be seen that the MOIHBA algorithm outperforms the other algorithms in terms of running time. This remarkable result confirms the positive and significant effect of using MOIHBA to solve MORPO problems.

V. CONCLUSION

In this research, to address the MORPO problem, an improved multi-objective honey badger algorithm, MOIHBA, is proposed. It includes an initialization process based on the sine chaotic mapping strategy as well as a backward learning mechanism, and a search process based on the cross-learning mechanism. Meanwhile, this paper obtains the pareto optimal set by using a method based on crowding distance and fast non-dominated ranking. To test the effectiveness and superiority of this method, the MOIHBA and three other algorithms are adopted to optimize the dual-objective and triple-objective reactive power optimization problems on three test systems of different scales, two evaluation indexes GD and HV and the average running time of the algorithm are adopted to analyze the comprehensive performance of different algorithms. The simulation results of each case and the analysis results of the evaluation indicators show that,

compared with other algorithms, the quality of the solution set and the comprehensive performance of the MOIHBA algorithm are superior. Therefore, the method proposed in this paper can be effective in solving the MORPO problem and has excellent theoretical and practical value.

REFERENCES

[1] D. O. Sidea, I. I. Picioroaga, A. M. Tudose, C. Bulac and I. Tristiu, "Multi-Objective Particle Swarm Optimization Applied on the Optimal Reactive Power Dispatch in Electrical Distribution Systems," in *2020 International Conference and Exposition on Electrical and Power Engineering (EPE)*, 2020, pp. 413-418.

[2] X. Liu, P. Zhang, H. Fang and Y. Zhou, "Multi-Objective reactive power optimization based on improved particle swarm optimization with ε-Greedy strategy and pareto archive algorithm," *IEEE Access*, vol. 9, pp. 65650-65659, 2021.

[3] G. Chen, J. Qian, Z. Zhang and S. Li, "Application of modified pigeon-inspired optimization algorithm and constraint-objective sorting rule on multi-objective optimal power flow problem," *Applied Soft Computing*, vol. 92, article. 106321, 2020.

[4] K. Ayan and U. Kılıç, "Artificial bee colony algorithm solution for optimal reactive power flow," *Applied Soft Computing*, vol. 12, no. 5, pp. 1477-1482, 2012.

[5] M. Basu, "Multi-objective optimal reactive power dispatch using multi-objective differential evolution," *International Journal of Electrical Power & Energy Systems*, vol. 82, pp. 213-224, 2016.

[6] M. Inoue, T. Sadamoto, M. Arahata and A. Chakrabortty, "Optimal power flow design for enhancing dynamic performance: Potentials of reactive power," *IEEE Transactions on Smart Grid*, vol. 12, no. 1, pp. 599-611, 2021.

[7] C. Zhang, Q. Liu, S. Huang, *et al.*, "Reactive power optimization under interval uncertainty of renewable power generation based on a security limits method," *International Journal of Electrical Power & Energy Systems*, vol. 130, article. 106894, 2021.

[8] M. K. Mangoli, K. Y. Lee and Young Moon Park, "Optimal real and reactive power control using linear programming," *Electric Power Systems Research*, vol. 26, no. 1, pp. 1-10, 1993.

[9] S. Duman, U. Güvenç, Y. Sönmez and N. Yörükeren, "Optimal power flow using gravitational search algorithm," *Energy Conversion and Management*, vol. 59, pp. 86-95, 2012.

[10] M. Rezaei Adaryani and A. Karami, "Artificial bee colony algorithm for solving multi-objective optimal power flow problem," *International Journal of Electrical Power & Energy Systems*, vol. 53, pp. 219-230, 2013.

[11] B. Zhao, C. X. Guo. and Y. J. Cao, "A multiagent-based particle swarm optimization approach for optimal reactive power dispatch," *IEEE Transactions on Power Systems*, vol. 20, no. 2, pp. 1070-1078, 2005.

[12] L. Lian, "Reactive power optimization based on adaptive multi-objective optimization artificial immune algorithm," *Ain Shams Engineering Journal*, vol. 13, no. 5, article. 101677, 2022.

[13] M. A. M. Shaheen, H. M. Hasanien and A. Alkuhayli, "A novel hybrid GWO-PSO optimization technique for optimal reactive power dispatch problem solution," *Ain Shams Engineering Journal*, vol. 12, no. 1, pp. 621-630, 2021.

[14] A. Attia, R. A. El Sehiemy and H. M. Hasanien, "Optimal power flow solution in power systems using a novel Sine-Cosine algorithm," *International Journal of Electrical Power & Energy Systems*, vol. 99, pp. 331-343, 2018.

[15] G. Chen, L. Liu and S. Huang, "Enhanced GSA-Based optimization for minimization of power losses in power system," *Mathematical Problems in Engineering*, vol. 2015, pp. 1-13, 2015.

[16] M. Mehdinejad, B. Mohammadi-Ivatloo, R. Dadashzadeh-Bonab and K. Zare, "Solution of optimal reactive power dispatch of power systems using hybrid particle swarm optimization and imperialist competitive algorithms," *International Journal of Electrical Power & Energy Systems*, vol. 83, pp. 104-116, 2016.

[17] N. H. Awad, M. Z. Ali, R. Mallipeddi and P. N. Suganthan, "An efficient Differential Evolution algorithm for stochastic OPF based active – reactive power dispatch problem considering renewable generators," *Applied Soft Computing*, vol. 76, pp. 445-458, 2019.

[18] D. Danalakshmi., R. Gopi., A. Hariharasudan, *et al.*, "Reactive power optimization and price management in microgrid enabled with blockchain," *Energies*, vol. 13, no. 23, article. 6179, 2020.

[19] C. Zhang, K. Zhou, S. Ye and A. M. Zain, "An improved cuckoo search algorithm utilizing nonlinear inertia weight and differential evolution for function optimization problem," *IEEE Access*, vol. 9, pp. 161352-161373, 2021.

[20] S. B. Raha, K. K. Mandal and N. Chakraborty, "Hybrid SMES based reactive power dispatch by cuckoo search algorithm," *IEEE Transactions on Industry Applications*, vol. 55, no. 1, pp. 907-917, 2019.

[21] R. N. Kalaam, S. M. Muyeen, A. Al Durra, H. M. Hasanien and K. Al Wahedi, "Optimisation of controller parameters for grid-tied photovoltaic system at faulty network using artificial neural network-based cuckoo search algorithm," *IET Renewable Power Generation*, vol. 11, no. 12, pp. 1517-1526, 2017.

[22] Y. Liu, D. Ćetenović, H. Li, E. Gryazina and V. Terzija, "An optimized multi-objective reactive power dispatch strategy based on improved genetic algorithm for wind power integrated systems," *International Journal of Electrical Power & Energy Systems*, vol. 136, article. 107764, 2022.

[23] J. Qian, P. Wang, C. Pu and G. Chen, "Joint application of multi-object beetle antennae search algorithm and BAS-BP fuel cost forecast network on optimal active power dispatch problems," *Knowledge-Based Systems*, vol. 226, article. 107149, 2021.

[24] K. Deb, A. Pratap, S. Agarwal and T. Meyarivan, "A fast and elitist multiobjective genetic algorithm: NSGA-II," *IEEE Transactions on Evolutionary Computation*, vol. 6, no. 2, pp. 182-197, 2002.

[25] R. Jamal, B. Men and N. H. Khan, "A novel nature inspired Meta-Heuristic optimization approach of GWO optimizer for optimal reactive power dispatch problems," *IEEE Access*, vol. 8, pp. 202596-202610, 2020.

[26] J. Zhang, X. Wang and L. Ma, "An optimal power allocation scheme of microgrid using grey wolf optimizer," *IEEE Access*, vol. 7, pp. 137608-137619, 2019.

[27] K. Sathish Kumar and T. Jayabarathi, "Power system reconfiguration and loss minimization for an distribution systems using bacterial foraging optimization algorithm," *International Journal of Electrical Power & Energy Systems*, vol. 36, no. 1, pp. 13-17, 2012.

[28] F. A. Hashim, E. H. Houssein, K. Hussain, M. S. Mabrouk and W. Al-Atabany, "Honey Badger Algorithm: New metaheuristic algorithm for solving optimization problems," *Mathematics and Computers in Simulation*, vol. 192, pp. 84-110, 2022.

[29] F. Islam, H. Hasanien, A. Al-Durra and S. M. Muyeen, "A new control strategy for smoothing of wind farm output using short-term ahead wind speed prediction and Flywheel energy storage system," in *2012 American Control Conference (ACC)*, IEEE, 2012, pp. 3026-3031.

[30] M. Nasouri Gilvaei, H. Jafari, M. Jabbari Ghadi and L. Li, "A novel hybrid optimization approach for reactive power dispatch problem considering voltage stability index," *Engineering Applications of Artificial Intelligence*, vol. 96, article. 103963, 2020.

[31] S. Abbasbandy, "Improving Newton–Raphson method for nonlinear equations by modified Adomian decomposition method," *Applied Mathematics and Computation*, vol. 145, no. 2-3, pp. 887-893, 2003.

[32] M. Ghasemi, S. Ghavidel, M. M. Ghanbarian and A. Habibi, "A new hybrid algorithm for optimal reactive power dispatch problem with discrete and continuous control variables," *Applied Soft Computing*, vol. 22, pp. 126-140, 2014.

[33] L. Jebaraj and S. Sakthivel, "A new swarm intelligence optimization approach to solve power flow optimization problem incorporating conflicting and fuel cost based objective functions," *e-Prime - Advances in Electrical Engineering, Electronics and Energy*, vol. 2, article. 100031, 2022.

[34] M. Sakawa, H. Yano and T. Yumine, "An interactive fuzzy satisficing method for multiobjective Linear-Programming problems and its application," *IEEE Transactions on Systems, Man, and Cybernetics*, vol. 17, no. 4, pp. 654-661, 1987.

[35] T. Dokeroglu, E. Sevince, T. Kucukyilmaz and A. Cosar, "A survey on new generation metaheuristic algorithms," *Computers & Industrial Engineering*, vol. 137, article. 106040, 2019.

[36] K. Y. Lee, Y. M. Park and J. L. Ortiz, "A united approach to optimal real and reactive power dispatch," *IEEE Power Engineering Review*, vol.PER-5, no. 5, pp.42-43, 1985.

[37] O. Alsac and B. Stott, "Optimal load flow with Steady-State security," *IEEE Transactions on Power Apparatus and Systems*, vol. PAS-93, no. 3, pp. 745-751, 1974.

[38] G. Chen, L. Liu, P. Song and Y. Du, "Chaotic improved PSO-based multi-objective optimization for minimization of power losses and L index in power systems," *Energy Conversion and Management*, vol. 86, pp. 548-560, 2014.

[39] G. Chen, L. Liu, Z. Zhang and S. Huang, "Optimal reactive power dispatch by improved GSA-based algorithm with the novel strategies to handle constraints," *Applied Soft Computing*, vol. 50, pp. 58-70, 2017.

[40] G. Chen, J. Cao and Z. Zhang, "Application of global best imperialist competition algorithm for multi-objective reactive power

optimization," in *2018 Chinese Automation Congress (CAC),* IEEE, 2018, pp. 1240-1245.

[41] G. Chen, J. Cao, Z. Zhang and Z. Sun, "Application of imperialist competitive algorithm with its enhanced approaches for multi-objective optimal reactive power dispatch problem," Engineering Letters, vol. 27, no.3, pp. 579-592, 2019.

[42] G. Chen, H. Zhuo, X. Hu, F. Long and H. Long, "Environment Economic Power Dispatch from Power System Based on Multi-objective Novel Tree Seed Optimization Algorithm," *IAENG International Journal of Computer Science*, vol. 48, no. 4, pp. 845-861, 2021.